LA-4595-MS

LOS ALAMOS SCIENTIFIC LABORATORY
of the
University of California

LOS ALAMOS • NEW MEXICO

Quarterly Status Report on the

Advanced Plutonium Fuels Program

October 1-December 31, 1970

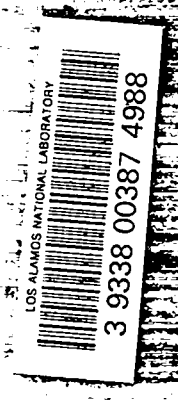

UNITED STATES
ATOMIC ENERGY COMMISSION
CONTRACT W-7405-ENG 36

This LA. . .MS report presents the status of the LASL Advanced Plutonium Fuels Program. Previous Quarterly Status Reports in this series, all unclassified, are:

LA-3607-MS	LA-3760-MS*	LA-4073-MS	LA-4376-MS
LA-3650-MS	LA-3820-MS	LA-4114-MS	LA-4437-MS
LA-3686-MS	LA-3880-MS	LA-4193-MS	LA-4494-MS
LA-3708-MS*	LA-3933-MS	LA-4284-MS	LA-4546-MS
LA-3745-MS	LA-3993-MS	LA-4307-MS	

This report, like other special-purpose documents in the LA. . .MS series, has not been reviewed or verified for accuracy in the interest of prompt distribution.

*Advanced Reactor Technology (ART) series.

Distributed: January 1971

LA-4595-MS
SPECIAL DISTRIBUTION

LOS ALAMOS SCIENTIFIC LABORATORY
of the
University of California
LOS ALAMOS • NEW MEXICO

Quarterly Status Report on the

Advanced Plutonium Fuels Program

October 1-December 31, 1970

FOREWORD

This is the 18th quarterly report on the Advanced Plutonium Fuels Program at the Los Alamos Scientific Laboratory.

Most of the investigations discussed here are of the continuing type. Results and conclusions described may therefore be changed or augmented as the work continues. Published reference to results cited in this report should not be made without obtaining explicit permission to do so from the person in charge of the work.

TABLE OF CONTENTS

PROJECT			PAGE
401	EXAMINATION OF FAST REACTOR FUELS		1
	I.	Introduction	1
	II.	Equipment Development	1
	III.	Hot Cell Facility at DP West	4
	IV.	Methods of Analysis	6
	V.	Requests from DRDT	8
	VI.	References	9
463	CERAMIC PLUTONIUM FUEL MATERIALS		10
	I.	Introduction	10
	II.	Synthesis and Fabrication	10
	III.	Irradiation Testing	10
	IV.	Properties	13
	V.	Publications	21
	VI.	References	21
472	ANALYTICAL STANDARDS FOR FAST BREEDER REACTOR OXIDE FUEL		22
	I.	Introduction	22
	II.	FFTF Analytical Chemistry Program	22
	III.	Neutron Capture Cross Section Values for Fission Products in Fast Reactor Spectra	23
	IV.	Investigation of Methods	24
	V.	Publications	28
	VI.	References	28

PROJECT 401

EXAMINATION OF FAST REACTOR FUELS

Person in Charge: R. D. Baker
Principal Investigators: J. W. Schulte
K. A. Johnson
G. R. Waterbury

I. INTRODUCTION

This project is directed toward the examination and comparison of the effects of neutron irradiation on LMFBR Program fuel materials. Unirradiated and irradiated materials will be examined as requested by the Fuels and Materials Branch of DRDT. Capabilities are established for providing conventional pre-irradiation and post-irradiation examinations. Additional capabilities include less conventional properties measurements which are needed to provide a sound basis for steady-state operation of fast reactor fuel elements, and for safety analysis under transient conditions.

Analytical chemistry methods that have been modified and mechanized for hot cell manipulators will continue to be applied to the characterization of irradiated fuels. The shielded electron microprobe and emission spectrographic facilities will be used in macro and micro examinations of various fuels and clads. In addition, new capabilities will be developed with emphasis on gamma scanning and analyses to assess spatial distribution of fuel and fission products.

High temperature properties of unirradiated LMFBR fuel materials are now being determined by Contractor in an associated project (ident No. 07463). Equipment designs and interpretive experience gained in this project are being extended to provide unique capabilities such as differential thermal analysis, melting point determination, high temperature dilatometry, and high temperature heat content and heat of fusion for use on irradiated materials.

II. EQUIPMENT DEVELOPMENT

A. Inert Atmosphere Systems

(C. E. Frantz, D. D. Jeffries, P. A. Mason, R. F. Velkinburg, L. A. Waldschmidt)

1. Disassembly Cell. The Ar atmosphere in the disassembly cell was maintained continuously during this Quarter by use of a recirculating purifier system for removing O_2 and H_2O. A 2 cfh Ar purge of the cell was maintained to hold the N_2 concentration to less than 1% by volume. Typical readings during this report period ranged from 4.5 to 15 ppm O_2 and 0.5 to 1.0 ppm H_2O.

2. Metallography Cells. The two metallography cells, and the metallographic blister were shut down during the last week of October and the first week of November for clean-up in preparation for locating and correcting leaks in the containment boxes. Large leaks were located at the manipulator ports of both cells. Smaller leaks were located at: the 7 in. and 18 in. transfer ports; viewing window seals; bolted panel seals; and flanges and weld joints of the intercell transfer tubes between the metallography cells and between the polishing cell and the blister. All leaks were sealed except those at the viewing window seals and the transfer tube between the polishing cell and the blister which were inaccessible without removing the alpha boxes from the cells. The manipulator port leaks were found to be caused by the center of gravity of the manipulators being located beyond the outermost set of support rollers on the through-tube, resulting in the slave end of the through-tube pivoting up against the top of the boot seal collar and

producing a gap around the bottom side of the through-tube seal. A temporary repair was achieved by placing a 1/8 in. shim under the through-tube at the master end. A more satisfactory and permanent solution will require ballasting the slave end of the manipulators sufficiently to shift the center of gravity to a point between the sets of support rollers or possibly using a top roller on the slave end of the through-tube.

After the leaks were sealed, concentrations of 30 ppm O_2 in the grinding cell and 95 ppm O_2 in the polishing cell were achieved with 40 cfh Ar purges. Levels on these boxes as low as 1.5 ppm O_2 and 0.5 ppm H_2O were attained during recirculation through the U. S. Dynamics purifier system with typical readings of <5 ppm O_2 and <1 ppm H_2O being observed. Operations in the metallography cells were resumed on November 12. Due to the urgency of resuming operations, the repair of a leak discovered in the boot of the blister manipulator was postponed until the next possible break in the operation schedule.

An attempt to minimize the use of Ar by reducing the purge flow for regenerating the moisture-gettering chemicals resulted in high H_2O readings in the metallography cells. A minimum of 40 cfh Ar purge flow appears to be necessary for efficient regeneration of the chemical.

3. Repair of Purifier. It has frequently been necessary to remove the U. S. Dynamics purifier (the unit used on the two metallography cells) from service to repair leaks. It is believed that the leaks are caused by corrosion from HCl and HF which were probably formed from the decomposition of Freon TF (CCl_2FCClF_2), a solvent used as both a grinding vehicle and as a cleaner in the ultrasonic tanks. Solid corrision products were analyzed and shown to be primarily $FeCl_2 \cdot X H_2O$. Deposits of this material plugged the inlet screen to the chemical tank.

The tanks were disassembled and the chemical absorbents removed prior to flushing the system with hot water to remove the corrosion products. It may be necessary to replace the corroded tanks with a more resistant material.

A search was initiated to find suitable replacement solvents for Freon TF to prevent future corrision to the Ar purifier system. Of the many solvents tested, n-butyl acetate satisfied most of the metallographic, chemical and safety requirements. This solvent has been used successfully for several weeks, but a much longer trial period will be needed to establish a true performance.

B. Sealed Manipulators
(P. A. Mason, C. D. Montgomery, R. F. Velkinburg)

The adapter wall tubes for the newly purchased CRL Model "L" manipulators have been fabricated. These will soon be fitted with necessary tubing and plumbing to accommodate the Ar purge pressure. A design is in process to develop a closed system type of purge for the Model "L" manipulator boots. The purge gas would be tapped from the alpha box purifier recirculation pump outlet and fed through an absolute filter, check valve and flow meter to the boot. The boot seal collar would incorporate an orifice to allow the purge gas to be vented into the alpha box and maintain the desired positive pressure differential between the boot and the alpha box atmosphere. A much higher purge flow could be tolerated ($\sim$ 20 cfh) with less likelihood of losing the positive pressure in a boot due to a tear than with the present system using a minimum flow, once-through purge. A back-up Ar supply would be activated by a "photohelic" pressure controller should the normal supply fall below a pre-set limit. The Ar supply through the boots would also serve as an adequate purge for the alpha box, and additional Ar would only be required to: (1) restore pressure, referred to above: (2) maintain the desired minimum concentration of N_2; and (3) regenerate chemicals in the purifier system.

C. Thermal Diffusivity
(M. E. Lazarus, R. F. Velkinburg)

Several changes have been incorporated in the thermal diffusivity furnace by the factory, and rechecking the furnace should be completed in January 1971.

D. In-Cell Equipment
(F. J. Fitzgibbon, M. E. Lazarus, P. A. Mason, C. D. Montgomery)

1. Sodium Distillation Apparatus. The new unit for removing Na from sections of fuel pins has been

designed and constructed. The diffusion pump remains to be incorporated into the system. The thermocouples and heating element have been tested and perform as expected.

2. Micro-Sampling System. Design of the injection mold for the metallographic mounts has been completed. It is hoped that one mount design can serve for metallography, 2-dimensional gamma scanning of a disc, and for micro-sampling operations.

Several samples of material (Noryl plastic) have been received for testing with radiation, solvents, acids, and in grinding and polishing operations.

3. Sealed Tube System for Chemical Dissolution

In cooperation with the Analytical Chemistry Group a sealed tube method for the dissolution of fuel samples is being adapted for remote operation. The principal items (listed below) of the remote system have now been designed and the fabrication is 85% completed.

a. A high pressure, high temperature furnace to accomplish the rapid dissolution of samples in acid within a sealed quartz tube. The furnace can be pressurized to 4000 psi and can attain a temperature of 300°C.

b. A powered, rotation fixture for flame-sealing the tube and for scribing the surface prior to opening.

c. A fracturing anvil for advancing the scribed ring on the quartz tube to a complete fracture for opening the tube.

d. A 4000 psi Ar supply system with attendant controls, safety devices, filter and pressure release.

e. Cooling water supply for the furnace and a gas supply for the heating torch on the sealing fixture.

The in-cell equipment for this system is nearly complete and is in process of proof test in mock-ups outside the hot cell. The external utilities are ~ 95% complete and it is anticipated that the installation will be completed and ready for use in late January.

E. New Metallograph Installation
(C. E. Frantz, K. A. Johnson, C. D. Montgomery, T. Romanik, R. F. Velkinburg)

1. Mini-Manipulators. The min-manipulator which was returned to the vendor because of damage in shipment has been returned, tested, and placed along with the other mini-manipulator into the new blister mock-up.

2. Leitz Metallograph. The new Leitz remote metallograph was moved to an unclassified area in November for further check-out and alignment by factory representatives. It was then returned to the mock-up area. Bench tests of this metallograph were quite satisfactory.

3. Alpha Containment Box. The design for the new blister box is nearly completed. It accommodates the Leitz metallograph, and B and L metallograph, ion etcher, several viewing ports and glove ports, a bag-out port, a main viewing window, a transfer system entry, two mini-manipulators, and space for possible future installation of an image analyzer head. Provision will also be made for a recirculating inert atmosphere system. It is expected that shop fabrication will start soon on this box.

4. Ion Etcher. The major interfacing components of the ion etcher are on hand and will be partially checked out in the mock-up box.

5. Image Analyzer. The Quantimet image analyzer was received during this report period and checked by a factory engineer. Recent bench tests indicate that this unit is performing satisfactorily.

F. Metallography Techniques
(J. H. Bender, C. E. Frantz, D. D. Jeffries, K. A. Johnson, P. A. Mason, L. A. Waldschmidt)

Efforts were made to obtain maximum compatibility of all the system components consisting of the specimens, metallographic quality, lubricants, diamond grit bonding agents, ultrasonic cleaning solutions, and the recirculating inert gas system. The following procedures are now in use on a long term trial basis:

Grinding stages - butyl acetate is used as both a lubricant and in the ultrasonic cleaners

Polishing stages - "Hyprez" is used as a lubricant. Butyl acetate is employed in the ultrasonic cleaners. Pentane is used as the final rinse.

After several weeks operation, this system appears to be producing the desired results. It is very effective, in combination with the high quality inert atmosphere, in preserving the rather reactive fission product depositions or interactions at the fuel-clad interfaces.

Sodium-logging of fuel in either failed elements or sodium bonded elements has been a continuing metallographic problem even in a high purity inert gas atmosphere. The problem has been somewhat solved by the following technique. The mounted, polished sample of sodium-logged material is placed in a beaker, covered with ethyl alcohol, and then placed in the vacuum chamber. A vacuum is applied three times followed by pressurization with Ar each time. The specimen is left in the alcohol for about 25 min at a pressure of -0.5 atmosphere. Ad additional cycle of 3 evacuations and pressurizations is carried out before the mount is removed from the vacuum chamber. This technique provides specimens that may be examined for several days before sodium-induced artifacts appear on the polished surface.

G. Scanning Electron Microscope
(K. A. Johnson)

This unit has been installed at the DP Site and is in operation. The non-dispersive energy analyzer and fast scan system have also been made operational.

H. Miscellaneous
(C. D. Montgomery, J. W. Schulte)

Shipping Casks

The design of the cask proposed to ship small sections of irradiated fuel pins has been submitted for approval by ALO and DOT. When the approval is received, fabrication will start immediately.

It is anticipated that sufficient fuel pins will be removed from the EBR-II Reactor over the next several years to justify the procurement of a second shipping cask. Consequently, the drawings from which Cask DOT SP 5885 was built are being upgraded to reflect recent minor design changes. It may not be necessary to submit the new design for approval by DOT, in which case fabrication of certain components could begin in early February.

III. HOT CELL FACILITY AT DP WEST

(F. J. Fitzgibbon, C. E. Frantz, M. E. Lazarus, C. D. Montgomery, J. R. Phillips, J. R. Trujillo)

The status of the major systems at the modified DP West Facility are listed below.

A. Structures and Building Equipment

1. All large hoists have been installed and tested. The auxiliary "high-lift" hoist to be mounted on the crane in the corridor is in fabrication and will be installed in February. The newly installed 25-ton hoist being used to lift a 21-ton fuel element cask is shown in Fig. 401-1. Criticality studies indicate that the casks, shown in Fig. 401-1, may be safely used for transporting 25 fast reactor fuel elements. Up to 36 fuel elements may be shipped safely by using boron-poisoned inserts.
2. Approximately 100 h each of electrical work and painting remain to be completed before the facility is released to the operating

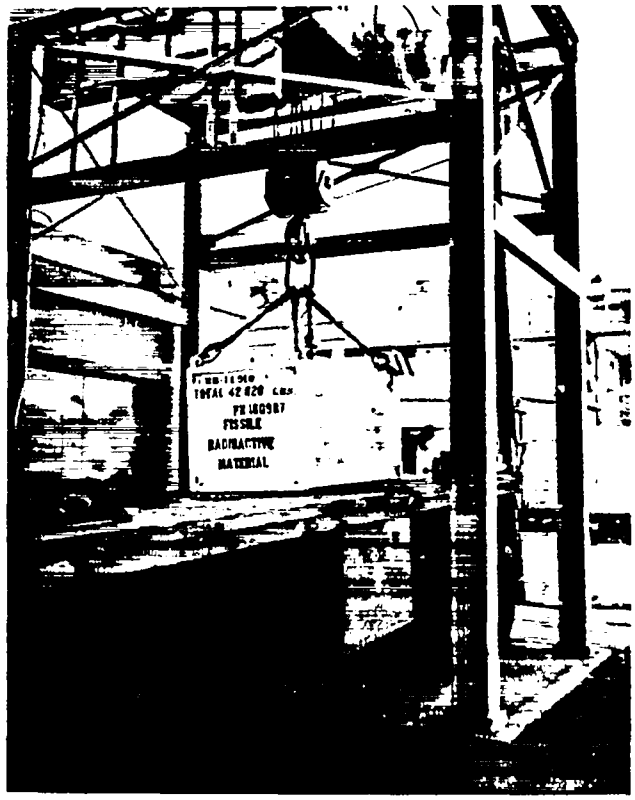

Fig. 401-1 25-Ton Hoist at DP West Hot Cell Facility

personnel. It is expected that this work also will be completed by the end of February.

3. The adapters for the storage holes, capable of storing 61-in.-long fuel elements, will be completed in February. Criticality studies show that as many as 25 fuel elements in each of the 4 cells and 25 elements in each of the 22 holes may be stored simultaneously without incurring a criticality risk.
4. The 23-ton capacity cart for moving casks between the hot cell corridor and the 25-ton hoist station is shown in Fig. 401-2. It is proposed to push (or pull) the cask between stations with the fork lift, also shown in Fig. 401-2. Tests were made in which the cart, loaded with 22 tons, was moved forward 40 feet and then returned to the starting point. The cart retraced to within 1/4 inch of the starting point, which is within specifications.

B. Hot Cell Equipment

1. Gamma Scanning System. The mechanical equipment for this system has been moved to the area where the fuel elements are temporarily being scanned. The equipment is undergoing final adjustments and check-outs in conjunction with the Nuclear Data 50/50 system.

Additional collimators are being fabricated for the new system.

2. Fission Gas Sampling System. Figure 401-3 shows the fission gas sampling system that will be installed at DP West. The fuel element drill is at the left of the figure with the drill motor below. To the right of this is the Baratron pressure sensing head and remote isolation valves, followed by the sample flask and calibration system, and finally the Baratron read out unit.

3. Macrophotography. The Quartz-Iodine lights that were to be used for illuminating the pin, produce too much heat and insufficient light. Therefore, a Xenon flash tube system is now being constructed for lighting the front of the pin. Figure 401-4 shows the equipment, which is complete except for the new front lighting. The camera assembly is on the left, and the lighting-pin positioning assembly on the right. The system should be complete by February 1.

4. Profilometer. A better lighting system is necessary for the profilometer to eliminate errors caused by pin motion in the front to back and side motions. Tests were run on Laser light sources and high intensity Xenon-Arc lamps and the results indicate that a Xenon-Arc lamp will supply the correct type of lighting. A purchase order has been issued for this type of lamp. The

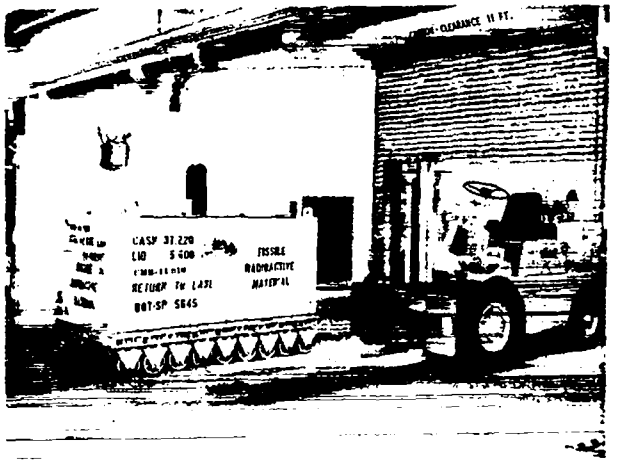

Fig. 401-2. Cask, Cart, and Fork Lift for use at DP West Hot Cell Facility

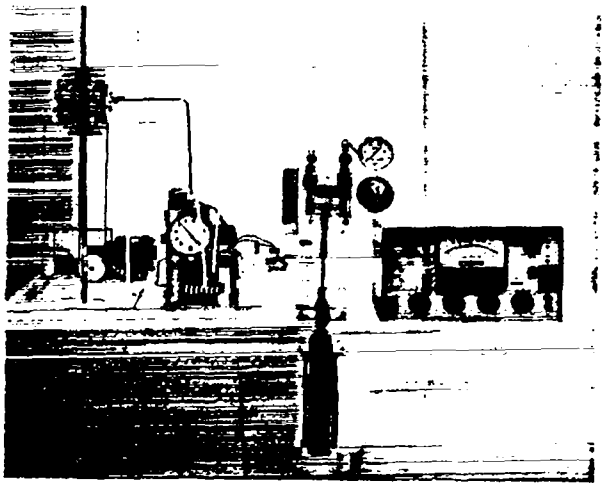

Fig. 401-3. Fission Gas Sampling System for DP West Facility

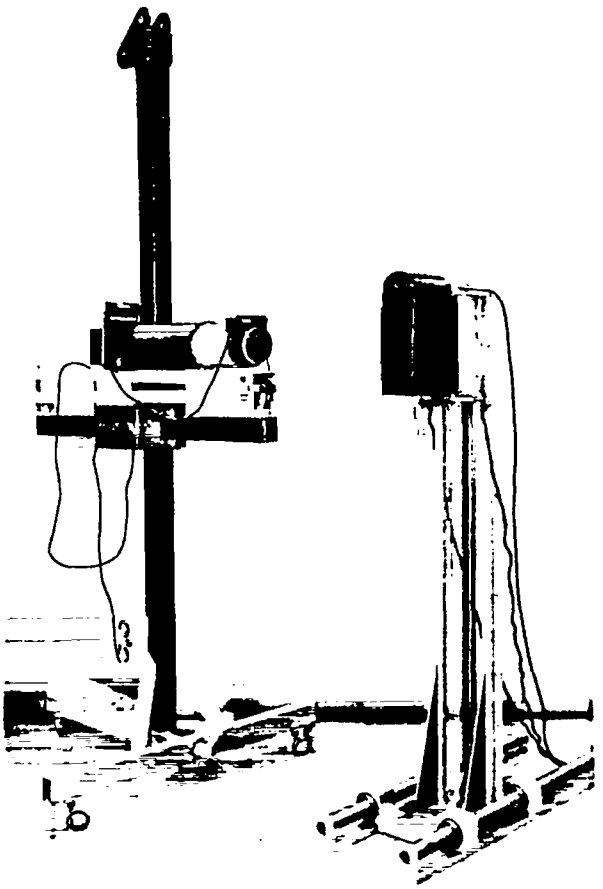

Fig. 401-4 Macrophotography System

system has been tested with a standard and the present lighting, and gives an accuracy of ± 0.0002 in. with no extraneous pin motions. If front to back and side motions of the pin are introduced, an error of 0.0005 in. occurs for a pin motion of 0.005 in. The new light source should decrease this form of error considerably.

This system is complete with the exception of the new lighting and the data storage system; however data can presently be recorded using a strip chart recorder. Figure 401-5 shows the electro-optical sensor and positioning stand. The sensor is positioned to look directly into the profilometer wall periscope. Positioning must be done to better than ± 0.002 in. Figure 401-6 depicts the in-cell equipment. This equipment positions and moves the fuel pin in front of the viewing periscope and presents electrical signals to indicate the exact position and orientation of the fuel pin.

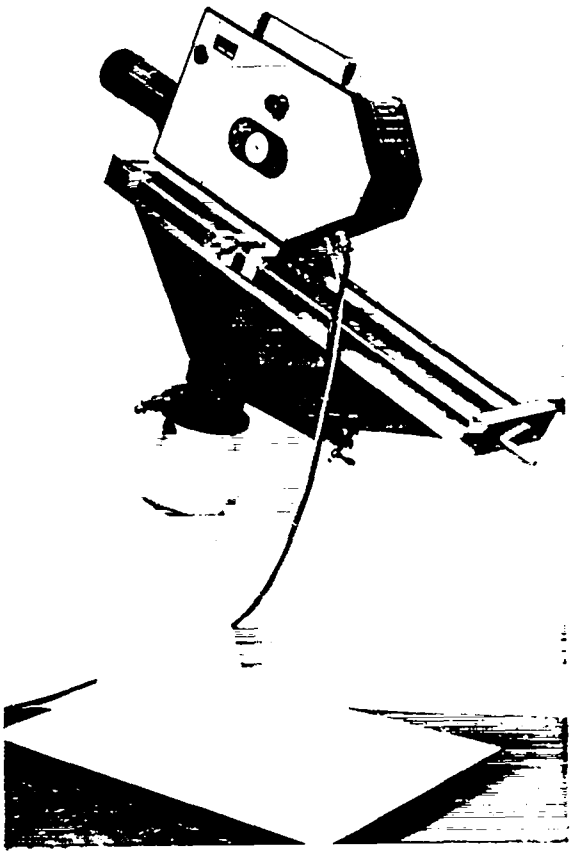

Fig. 401-5 Profilometer Electro-Optical Sensor and Stand

5. Sodium Dissolution. A system for removal and dissolution of sodium between the capsule and pin has been fabricated. A cover of inert gas is provided by a hood which fits over the dissolution tray.

IV. METHODS OF ANALYSIS

A. Measurement of U and Pu

(J. W. Dahlby and G. R. Waterbury)

Controlled-potential coulometric titrations of U and Pu in $(U,Pu)O_2$ fuels having undergone 6 at.% burnup showed that the U contents varied from 64.5 to 66.4% and the Pu contents from 16.9 to 17.4% among three samples from one fuel rod. As the precision (1 σ) of the repeated titrations were 0.3% for the U and 0.1% for the Pu measurements, the large ranges of concentrations for the two elements indicated either incomplete solution of the samples, variable amounts of Na in the fuel, or non-uniformity of the fuel itself.

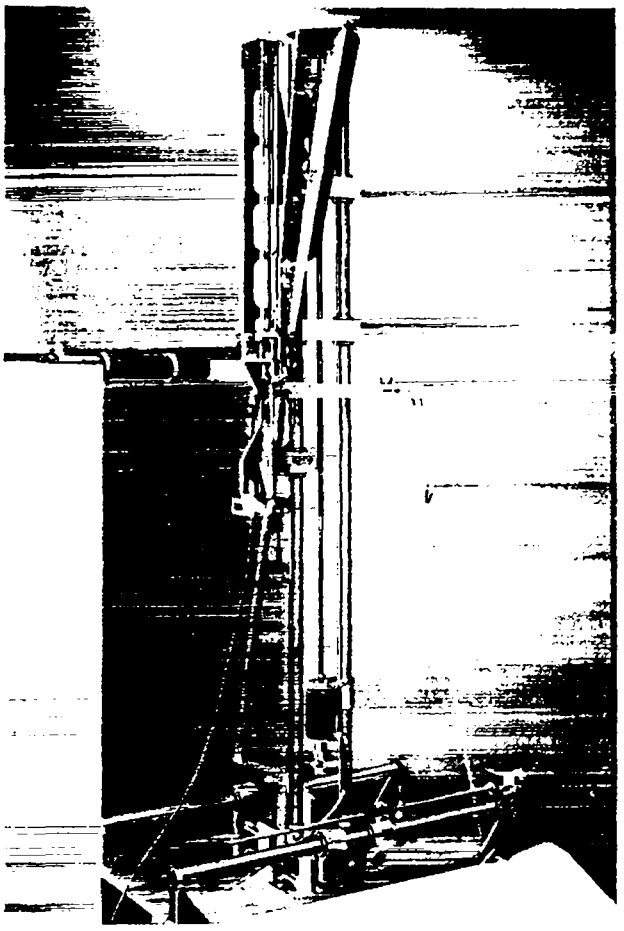

Fig. 401-6 In-Cell Profilometer Equipment

To determine if incomplete dissolution was the cause of the variances, two more samples of $(U_{0.8}Pu_{0.2})O_2$ from the same fuel element were dissolved quantitatively, and the U and Pu titrated repeatedly. Most of each sample was dissolved in hot HNO_3-HF followed by fusion of the insoluble residue in $KHSO_4$. The small amount of residue remaining was removed from the hot cell and dissolved at 325°C in HCl in a sealed tube.[1] Aliquots containing 3 mg of fuel (0.5 mg of Pu) from each final solution were analyzed for Pu, and aliquots containing 1 mg of fuel (0.6 mg of U) were titrated for U. For the Pu titrations, the currents for the coulometric oxidation of Pu(III) to Pu(IV) and for the reduction of Pu(IV) to Pu(III) at a Pt electrode were integrated. The oxidation and reduction cycles were repeated until consecutive values for Pu differed by less than 2 μg. The integrated current for the coulometric reduction of U(VI) to U(IV) at a Hg electrode, following a preliminary reduction of more-easily-reduced impurities, was used in calculating the U content. A second reduction on the same solution was made to obtain a titration blank caused by radiolysis. The results for the two samples were 64.7 ± 0.1% and 64.3 ± 0.2% U, and 17.6 ± 0.2 and 16.8 ± 0.1% Pu. As these samples were completely dissolved, it was obvious that the segregation in the fuel or some other factor caused the variations in the results. Variable amounts of Na in the fuel is considered the most likely cause. Fuel samples from a fuel pin not containing Na will be analyzed next.

An apparatus is being fabricated and installed in a hot cell to dissolve high-burnup fuel samples more rapidly by the sealed-tube technique.[1] Testing of this equipment will begin soon.

B. Determination of O_2 in Irradiated Fuels
(C. S. MacDougall and M. E. Smith)

An analytical system for measuring O_2 in various irradiated materials was tested by satisfactorily analyzing several U_3O_8 and irradiated stainless steel samples. In this system, the sample is reacted with C at 2000°C, and the CO and CO_2 produced are swept from the furnace by Ar and measured either gravimetrically or manometrically. Use of this system to measure O_2 in one irradiated $(U,Pu)O_2$ fuel sample was not satisfactory because of apparent low results. Additional measurements of O_2 in this fuel are being made to determine if this anomaly is real. It may be necessary to increase the reaction temperature or to use a longer collection time for the CO and CO_2. Tests are planned to establish optimum experimental conditions for the quantitative release of O_2 as CO and CO_2.

C. Gamma Scanning
(J. Phillips and G. Mottaz)

Areas of interest in irradiated fuel elements for further analyses and destructive sectioning are pinpointed by information gained by gamma scanning. To improve gamma scanning capabilities, a new gamma scanning system consisting of a Nuclear Data 50/50 data acquisition system, a Ge(Li) anticoincidence detector system, and a precision scanning mechanism has been assembled and operated satisfactorily. This system permits more

rapid gross gamma scanning and the automatic accumulation and reduction of data for up to 30 individual gamma photopeaks which may be used for either one-dimensional or two-dimensional high resolution gamma scans. The scanning mechanism has not yet been installed in the hot cell, and only low activity samples have been scanned in the initial operational tests. Installation of the scanning mechanism in a hot cell is in progress.

A computer code has been written to accept one or more diametral scans taken at different angles around the outside of a fuel element and to use this information in determining the radial distribution of each isotope of interest over a cross section of the fuel element. The calculated distribution is presented as an isometric projection plot and also as a density plot.

V. REQUESTS FROM DRDT

A. Examination of Irradiated Material

(K. A. Johnson, E. D. Loughran (GMX-2), R. A. Morris (GMX-1), J. R. Phillips, J. W. Schulte, G. R. Waterbury)

Los Alamos Scientific Laboratory: LASL Capsules 36B and 42B. Table 401-I outlines the tests and examinations made on these two capsules.

Metallographic examinations consisting of macrophotography, alpha and beta-gamma autoradiography, optical metallography and photograph mosaics are completed on 4 fuel-cladding and 1 cladding weld area specimens of 42-B. A fuel-cladding wafer approximately 0.050 in. thick was prepared in a special grinding apparatus for 2 dimensional gamma scanning.

TABLE 401-I
Post-Irradiation Examination of LASL Tests

	Examination	Capsule 36-B	Capsule 42-B
1.	Visual Inspection and Photography	x	x
2.	Measurements of Contamination and Radiation	x	x
3.	Measurement of Temperature (Capsule)	x	x
4.	Radiography	x	x
5.	Micrometer Measurement	x	x
6.	Gamma Scanning	x	x
7.	Analysis of Cover Gas in Capsule		x
8.	Analysis of Fission Gas in Pin		x
9.	Na Removal		x
10.	Clad Removal		x
11.	Center Point Balance		x
12.	Measurement of Temperature (Pin)		x
13.	Profilometry		x
14.	Sectioning in an Ar Atmosphere		x

A fuel specimen from 42-B was shipped to INC for burnup determination, and one sample was prepared for electron microprobe examination.

Measurements of density by immersion were made on a cladding section of 42-B.

OWREX Tests. Specimens, 1 each, were prepared from a fuel section and a stainless steel pellet of OWREX -15 for examination on the microprobe.

Following visual examination and radiography, an OWREX environmental chamber, reading about 40 rhm, was placed in the contaminated waste dump along with fuel and hardware from OWREX-11, -12, -13, -14, and -15.

Nuclear Materials and Equipment Corporation: A-Series Pins. Eleven pins, A-1 through A-11, were received on November 25. Tests performed thus far on these pins are shown tabulated below.

TABLE 401-II
Post-Irradiation Examination of NUMEC Materials

	Tests	NUMEC Pin No.
1.	Visual Inspection and Photography	A-1 through A-11
2.	Measurements of Contamination and Radiation	A-1 through A-11
3.	Measurements of Temperature	A-1 through A-11
4.	Center Point Balance	A-1 through A-11
5.	Betatron Radiography	A-1, A-2, A-3

Negotiations are being made with DRDT to provide ORNL and ANL with some of the A-Series materials following testing at LASL.

B-Series Pins. Specimens were removed from the B-1 and B-11 fuel sections for chemical development studies.

Two samples, obtained from the capsules used in the DTA experiments on B-9 fuel, were examined by macrophotography, alpha and beta-gamma autoradiography, and optical microscopy. One sample (B-9D) was then prepared for electron microprobe examination, and the examination was completed.

United Nuclear Corporation. Examination of 11 capsules or pins from UNC were made by performing tests shown in the following table.

TABLE 401-III

Post-Irradiation Examination of UNC Materials

Tests	UNC Experiment No.								
	92	96	99	104	107	108	109	111	112
1. Visual Inspection and Photography	x	x	x	x	x	x	x	x	x
2. Meas. of Contamination and Radiation	x	x	x	x	x	x	x	x	x
3. Meas. of Temperature (Capsule)	x	x	x	x	x	x	x	x	x
4. Radiography	x	x	x	x	x	x	x	x	x
5. Micrometer Measurements	x	x	x	x	x	x	x	x	x
6. Gamma Scanning	x	x	x	x	x	x	x	x	x
7. Analysis of Cover Gas in Capsule	x	x	x	x					
8. Clad Removal		x	x	x					
9. Center Point Balance	x	x	x	x	x	x	x	x	x
10. Na Removal		x	x	x					

Examination of the "rabbit irradiation" experiments was continued during this period. Temperature and profilometer measurements were completed on Pins UNC-210 through -221.

Two capsules (UNC-138 and UNC-146), scheduled for possible re-insertion in the EBR-II, were received on December 28. Preliminary contamination and temperature measurements were made prior to storage.

Metallographic examinations, including macrophotography, alpha and beta-gamma autoradiography and optical metallography, were completed on the UNC-125, -126, -127, and -128 specimens listed below.

TABLE 401-IV

Metallography of UNC Material

Element No.	No. of Specimens	
	Fuel-Cladding	Cladding
UNC-125	5	1
UNC-126	4	1
UNC-127	4	1
UNC-128	4	1

Fuel specimens from UNC-125H, -126H, -127C, and -127H were prepared for microprobe examinations, and the examinations of UNC-125H, -127C, and -127H were completed.

Fuel specimens from UNC-125 H, -126 H, -127 C, and -127H were prepared for microprobe examinations, and the examinations of UNC-125 H, -127 C, and -127 H were completed.

VI. REFERENCES

1. C. F. Metz and G. R. Waterbury, LA-3554, 1966.

PROJECT 463

CERAMIC PLUTONIUM FUEL MATERIALS

Person in Charge: R.D. Baker

Principal Investigator: J.L. Green

I. INTRODUCTION

This program has two primary goals. The first is the investigation of the irradiation behavior of well characterized LMFBR advanced fuel materials. These studies currently emphasize the evaluation of uranium-plutonium monocarbide compositions as candidate fast breeder fuels. A continuing series of irradiation experiments is being carried out under steady state conditions in fast reactor environments to assess the effects of damage and burnup on stainless steel clad, sodium bonded, monocarbide fuel elements. These experiments are designed to investigate fuel swelling, interactions between the fuel and clad and thermal bonding medium, fission gas release, and the migration of fuel material and fission products as a function of burnup and irradiation conditions. In addition, experiments are being designed to allow the study of the effects of rapid, overpower, reactor transients on sodium bonded monocarbide fuel assemblies. Contiguous efforts are necessary in the development of fuel material preparation and fabrication procedures as well as the techniques required for the characterization of fuel materials both before and after irradiation.

The second objective in the program is the determination of thermophysical, mechanical and chemical properties and characteristics of plutonium containing ceramics that are required for their evaluation and use as fuel materials. A broad range of capabilities in this area has been developed, including the study of (1) phase relationships using differential thermal analysis, (2) thermal transport, (3) thermal stability and compatibility, (4) hot hardness and its temperature dependence, (5) structure and phase relationships using high temperature x-ray and neutron diffraction, (6) thermal expansion, and (7) compressive creep rates as a function of temperature and stress.

II. SYNTHESIS AND FABRICATION

(R. Honnell, C. Baker, W. Hayes, G. Moore, and R. Walker)

As a continuing effort, carbide specimens of various compositions are being prepared and characterized for use in EBR-II irradiation assemblies and property measurements. A cursory study was completed on the occurrence of end capping and microcracking in chamfered (U, Pu)C fuel pellets. The results of this study indicate a defect occurrence of 10% or less in chamfered pellets pressed from powders slugged at 30 tsi, and a 40 to 50% rejection rate for pellets pressed from powders slugged at 10 tsi. At the present, all carbide fuel scheduled for irradiation testing is being fabricated with chamfered ends, using powders slugged at the higher pressure.

III. IRRADIATION TESTING

1. EBR-II Irradiation Testing

(J.O. Barner)

The purpose of the EBR-II irradiations is

the evaluation of candidate fuel/sodium/clad systems for the LMFBR program. In the reference design, fuel pellets of single-phase (U, Pu) C are separated by a sodium bond from a cladding of Type 316 stainless steel. Three series of experiments are planned for which approval-in-principle has been received from the AEC. The capsules are to be irradiated under the conditions shown in Table 463-I.

Results: Two capsules from Series 1, designated K-42B and K-36B, have been returned to the LASL hot cells for examination. Revised estimates of burnup from EBR-II are 5.0 at.% and 3.7 at.% for K-42B and K-36B respectively. Both capsules have completed the nondestructive phase of examination, which consists of neutron radiography at TREAT, Betatron radiography, and gamma scanning.

Neutron and Betatron radiographs show that all pellets in both capsules are split axially due to thermal stresses. Transverse cracks and general fragmentation were also observed in fuel pellets in both capsules. No indication of inner element failure was observed for either experiment.

Both capsules were gross gamma scanned with a 0.020 in. collimator in 0.015 in. steps over their entire length. All capsule components were found to be in their proper positions. The fuel stack height had expanded 2.15% and 2.25% for capsules K-42B and K-36B respectively. In the case of K-36B, there was a distinct drop in gamma activity at the top of pellet 53 as numbered from the bottom of the stack. This activity drop corresponds to a capped pellet which was observed in the radiograph. This partially accounts for the higher apparent stack height expansion for K-36B.

TABLE 463-I

EBR-II IRRADIATION CONDITIONS

Condition	Series 1	Series 2	Series 3
1. Lineal Power, kW/ft	~ 30	~ 45	~ 30
2. Fuel Composition	($U_{0.8}Pu_{0.2}$) C, single-phase, sintered)		
3. Fuel Uranium	^{235}U	^{233}U	^{235}U
4. Fuel density	90%	95%	95%
5. Smear density	80%	80%	80%
6. Clad size	0.300 in. i.d. x 0.010 in. wall		
7. Clad type	316 SS	316 SS	316 SS
8. Max clad temp, °F	1250	1275	1250
9. Max fuel centerline temp, °F	2130	2550	2100
10. Burnup	3 at.% to 8 at.%		

Both capsules were also gross gamma scanned over the fueled length with a 0.004 in. collimator in 0.003 in. steps. Computer printouts and plots were utilized to determine individual pellet length increases. The implied fuel swelling rates based on the maximum length change, assuming isotopic swelling, were 2.43 vol% per at.% burnup for K-36B, and 2.16 vol% per at.% burnup for K-42B. The burnup normalized average implied swelling rates for the total fuel stack heights were 2.03 vol% per at.% burnup for K-36B and 1.51 vol% per at.% burnup for K-42B. The fuel swelling rates in both capsules were higher in the high fuel temperature, high burnup region.

Axial multispectral gamma scans of both capsules were also completed. Data was obtained for ^{103}Ru, ^{134}Cs, ^{137}Cs, ^{95}Zr-^{95}Nb, and ^{140}La. No detectable preferential migration of any of the fission products was observed along the axis of the fuel.

Capsule 42B is currently being destructively examined. Analysis of a gas sample from the capsule annulus revealed no fission gas activity, indicating that the inner element had not failed.

Element profilometry was completed on four axial traverses. Some fuel-cladding mechanical interaction resulted in oval clad sections occurring on a 2 to 3 in. pitch. Very little mechanical deformation was observed that correlated with a pellet length pitch (~0.250in.). The maximum observed clad deformation was 0.0039 in. or 1.29% strain. The calculated fast neutron damage linear clad swelling[1] was 0.0017 in. or 0.58% strain. The maximum interaction was observed in the maximum burnup region.

The capsule K-42B element has been sectioned and samples taken for metallography, burnup and density measurements, pinpoint gamma scanning, microprobe analysis, scanning electron microscopy, α autoradiography, β-γ autoradiography, and sodium fission product chemistry.

Capsule K-36B will be returned to EBR-II for reinsertion after the K-42B analysis has been completed.

Three capsules from Series 1, designated K-37B, K-38B, and K-39B, and two capsules from Series 3, designated K-43 and K-44 are currently being irradiated in the EBR-II X086 subassembly at approximately 30 kW/ft. The target burnup for these capsules is 6 to 8 at.%.

The three capsules from Series 2, designated K-49, K-50, and K-51, and two additional capsules from Series 3, designated K-45 and K-46,are available at EBR-II for irradiation.

One thermal control capsule has been removed from a sodium loop after 6000 hours at 670°C. A second capsule will continue thermal exposure to 10,000 hours at 670°C.

Approval-in-principle for the irradiation of a singly-contained 19 pin subassembly of sodium-bonded carbides in EBR-II has been requested from DRDT.

2. Thermal Irradiations of Sodium-Bonded Mixed Carbides
(J. C. Clifford)

Sodium-bonded mixed carbides have been irradiated in the LASL Omega West Reactor, a 6 MW MTR-type facility, to determine whether fuel, clad, and sodium remain mutually compatible as burnups of interest to the LMFBR program are approached. Experimental conditions included fuel surface operating temperatures of 600 - 700°C, a fuel radial temperature gradient of 180°C, and fuel power densities varying from approximately 670 w/g at the surface to 50 w/g at the centerline. Experiments that reached approximately 4 and 8 at.% surface burnup have been examined destructively without revealing any significant deleterious effects on compatibility. A third and final experiment was operated successfully to an estimated 12 at.% surface burnup, and presently is awaiting destructive examination. Upon completion of this examination, a topical report will be prepared describing the experiments and their results.

3. Transient Overpower Testing of Sodium-Bonded (U, Pu)C
(J. C. Clifford, J. O. Barner, J. F. Kerrisk, D. G. Clifton, and R. E. Alcouffe)

The immediate objective of these tests is to determine the response of sodium-bonded mixed carbide fuel pins to transient overpower conditions. The tests are part of a larger program to evaluate the potential of this fuel concept for use in liquid metal cooled fast breeder reactors. Sodium-bonded carbides are expected to exhibit different transient behavior than do the gas-bonded oxides currently under investigation, primarily because of the higher thermal conductivities of the carbide fuel and sodium bond. In attempting to make analytical predictions of carbide pin response to transient overpower conditions, one principal uncertainty is the behavior of the bonding sodium, e.g., the degree of sodium superheat attained and the nature of sodium movement in the thin, irregularly shaped annulus between fuel pellets and cladding. For example, a transient severe enough to produce central melting of carbide fuel also may lead to clad melting if sodium is not expelled rapidly enough from the bond region.

Tests are being designed to probe sodium bond behavior, cladding deformation, fuel movement, and fuel-cladding interactions in a stepwise fashion, beginning with mild excursions expected to produce bond instabilities and extending to severe transients expected to cause fuel expulsion. It is anticipated that initial tests will be conducted in the Transient Reactor Test Facility (TREAT) and will employ defect-free, previously unirradiated , single pins. Future experiments can be extended to evaluate the effects of bond and cladding defects and of retained fission gas on fuel pin damage thresholds and failure mechanisms.

Neutronics Calculations on TREAT Carbide Experiments: Microscopic cross-section data for both the TREAT reactor and the plutonium carbide experiment capsule are being derived from the ENDF/B data file.[2] The data has been processed by the ETOX code[3] yielding a 30-group thermal set of data where the energy intervals are approximately equal in neutron speed. The epithermal data were evaluated at equal lethargies of 0.5 up to 3.5 keV, yielding 17 groups; seven more groups were added to account for the fast range. The 30-group thermal data were used by the GLEN code[4] to reduce the number of groups needed to five based on a TREAT cell spectrum with upscattering provided by a thermal graphite scatterer derived from ENDF/B.

This five-group thermal data, together with the epithermal and fast data, will be used in a DTF-IV calculation[5] of a one-dimensional model of the TREAT reactor and the experiment. This 29-group calculation will then be used to derive a one-thermal-group, 24-fast-group cross section set for both the reactor and the experiment. This derived set will then be used in two-dimensional calculations on the entire system to determine power ratios and flux profiles.

Particular attention has been paid to the epithermal region because it is anticipated that it will be necessary to neutronically filter the experiment. To accomplish this, boron will be placed between the reactor and the experiment, thereby reducing the thermal flux in the experiment. Therefore, the power in the experimental fuel will be produced mainly by epithermal neutrons.

TREAT Heat Transfer Calculations: Heat transfer calculations have been started to predict the behavior of (U, Pu)C fuels subject to energy generation transients. The calculations are aimed at simulating the behavior of sodium bonded fuel pins during transient tests in the TREAT reactor, and are being performed using the CINDA (Crysler Improved Numerical Differencing Analyser) code. The calculations use a one dimensional (radial) network with space and time dependent energy generation rates, temperature dependent properties, phase changes, and radiative heat transfer where appropriate.

Initial calculations were for a 0.262 in. diameter $(U_{0.8}Pu_{0.2})C$ fuel, sodium bonded to a 0.282 in. I.D. by 0.310 in. O.D. stainless steel cladding. A heat sink was sodium bonded to the outside of the clad. The following parameters were investigated:

1. Heat sink material - Na, Ni, Al
2. Space energy generation - uniform to flux depressions of 12 to 1
3. Time energy generation - step function and two typical TREAT transients[6]
4. Total energy deposited
5. Initial system temperature.

Two major differences, from the standpoint of heat transfer, between these tests and gas bonded oxide tests are the higher conductivity of the carbide fuel compared to the oxide and the higher conductivity of a sodium bond compared to a gas bond. Both conditions point to a larger fraction of the heat generated in the carbide fuel being lost to the clad and heat sink as long as the fuel-clad sodium bond remains liquid. The heat transfer calculations indicate that fuel melting and clad melting are initiated about the same time if the fuel-clad sodium bond is assumed to remain liquid. Large flux depressions shorten the time required to initiate clad melting. It is also possible that the fuel-clad sodium bond could be ejected when the sodium bond vapor pressure exceeds the fuel pin cover gas pressure. This second situation was simulated by replacing the liquid sodium bond with a sodium vapor bond above a prescribed temperature. Conduction through the sodium vapor and radiation from the fuel surface to the clad were allowed. The conductance of the vapor bond is about a factor of 40 less than the liquid. Thus, bond expulsion is followed by a rapid rise in fuel temperature and a drop in clad temperature. It is recognized that neither limiting assumption (bond remaining liquid or complete expulsion) provides an accurate picture of reality, but they do describe a range of possible test results which can be correlated with actual tests.

IV. PROPERTIES

1. Differential Thermal Analysis

(J.G. Reavis and L. Reese)

Differential thermal analysis measurements on irradiated UO_2 - 20% PuO_2 (NUMEC B-9-56) have been repeated with no significant change in observed solidus and liquidus temperatures. Additional DTA measurements have been made on samples in the Pu-C system. Investigations are currently being carried out which are directed toward the determination of the range of carbon composition of the single phase monocarbide phase field as a function of temperature. These studies will be limited to U/Pu ratios near 80/20, which is characteristic of LMFBR candidate fuels. A knowledge of these composition limits is essential to the systematic development of preparative procedures and is also important in the evaluation of the effect of carbide forming fission products on the physical and chemical properties of

irradiated carbide fuels.

DTA of Irradiated Samples: It was reported in the last quarterly report that a sample of UO_2 - 20% PuO_2 (NUMEC B-9-56) irradiated to a level of ~ 57,000 MWD/MTM had been sealed in a W capsule and observed using DTA. The capsule was sectioned and the cell and contents were examined using metallographic and electron microprobe techniques. It was found that significant quantities of Sn, Si, Ca and K were present in the polished sample. The time of introduction of these impurities is not known.

A second sample of the same irradiated oxide has been sealed in a W capsule and examined over the range 1300 - 2900°C. After DTA, the capsule was sectioned in the same manner as the first, but the entire sample was lost during the sawing operation so that no examination for impurities could be made.

A sample of unirradiated archival material from the same batch of UO_2 - 20% PuO_2 that was used to load fuel rod NUMEC B-9 was examined using the same equipment and techniques used with the irradiated specimens. Post-melting examination of the archival sample showed no indication of the impurities that were seen in the first sample of NUMEC B-9-56.

Results of DTA of the three samples are shown in Table 463-II.

TABLE 463 - II

RESULTS OF DTA OF UO_2 - 20% PuO_2 SAMPLES IN SEALED W CAPSULES

Sample	Solidus, °C	Liquidus, °C	Other, °C
NUMEC B-9, No. 1	2725±30	2825±30	2685±30
NUMEC B-9, No. 2	2740±25	2840±25	2685±25
Archival Mat'l.	2750±25	2840±25	None

The differences in the respective solidus and liquidus temperatures of the three samples are not believed to be significant. The only remaining difference between archival and irradiated oxide is the presence of a weak thermal arrest at 2685°C in the latter. This arrest was so weak that its existence was somewhat questionable, but the effect was observed several times in both irradiated samples. It may be a solidus or melting point involving fission products or other "impurity" phases.

When the magnitudes of the observed thermal arrests are considered, it is apparent that no appreciable melting of this oxide fuel occurs below 2725 ± 25°C at this burnup (~ 6.2%), but it is not possible to conclude from these observations that no liquid is present below this temperature. Indeed, some of the fission products probably have melted while others are present chiefly in the gas phase at the "solidus" temperature of the bulk fuel.

DTA of Pu-C Samples: Three compositions in the Pu-C system have been investigated using DTA and quenching techniques. These compositions and transformation temperatures are listed in Table 463-III. Transformation temperatures A through E are in good agreement with commonly accepted values of transformation temperatures of pure Pu metal. The nature of the thermal arrest F - F* may indicate a compositional range of homogeneity of zeta phase carbide which is in disagreement with the commonly accepted phase diagram.

Transformation G agrees rather well with published values of the Pu-PuC eutectic temperature. Transformation H for Pu agrees with reported melting points of pure Pu. Transformation H observed for $PuC_{0.33}$ and $PuC_{0.51}$ gives the location of the liquidus curve in this range of C concentration and aids in the extrapolation between the eutectic temperature and the previously-determined liquidus of $PuC_{0.9}$.

2. B_4C Structural Study
(K. L. Walters and J. L. Green)

Neutron and x-ray diffraction studies are being carried out on high purity samples of carbon saturated boron carbide in an attempt to more completely define

TABLE 463-III

TRANSFORMATION TEMPERATURES OF Pu-C SAMPLES

Composition	Transformation Temperatures, °C								
	A	B	C	D	E	F	F*	G	H
Pu	121	208	320	457	482	---	---	---	639
$PuC_{0.33}$	118	209	325	457	477	542	575	632	1500
$PuC_{0.51}$	121	208	323	458	476	546	577	634	1600

TABLE 463-IV

STRUCTURAL PARAMETERS FOR BORON CARBIDE *

Lattice Parameters	
Hexagonal	Rhombohedral
a_o = 5.6016 ± 0.0003 Å	a_o = 5.1625
c_o = 12.072 ± 0.001 Å	α = 65.65 deg.

Position Parameters (Hexagonal)		
	x	z
BI	0.839 ± 0.001	0.359 ± 0.001
BII	0.893 ± 0.002	0.114 ± 0.001
CI	-----	0.382 ± 0.001

Coherent Scattering Amplitudes (x 10^{12} cm)			
	Icosahedral Position	Terminal Chain Position	Central Chain Position
Preliminary Study[7]	0.522	0.665	0.535
Current Results	0.533±0.015	0.668±0.016	0.533±0.011
	Natural C 0.661		
	Natural B 0.54		

* All error limits are calculated 1σ limits uncorrected for covariance.

the crystallographic structure of that compound.

Final neutron diffraction data have been obtained and analyzed. Analytical data for the "B_4C" used in the preparation of the targets have been reported previously.[7] Peak intensity data for the neutron diffraction pattern have been least squares fitted to yield final values for both atomic position parameters and coherent scattering amplitudes for each crystallographic position in the structure. The results of these calculations are shown in Table 463-IV. Table 463-V shows a comparison of the results of this study with those from the original structure determination[8] in the rhombohedral coordinate system.

The position parameter results from the present study are not significantly different than those from the original determination. The identity of the atoms in each position are, as has been reported before,[7] not the same. Clark and Hoard identified all the atoms in the

TABLE 463-V

RHOMBOHEDRAL POSITION PARAMETERS

	Clark and Hoard[8]		Present Study	
	x	z	x	z
BI	0.193	0.693	0.198	0.684
BII	0.007	0.325	0.007	0.327
CI	0.385	---	0.382	---

icosahedral groups as B and all the atoms in the central chain as C. These assignments were presumptive in the sense that they were tailored to match the known stoichiometry of the compound. The authors stipulated that the differentiation between C and B was not possible from their data. The scattering amplitude results from the present study clearly indicate that the central 3 atom chain consists of two C atoms located on either side of a B atom, i.e., (CBC).

The chemical composition of the material used in the current study appears to require an overall stoichiometry of B_4C. The powder used in the neutron diffraction study contained excess carbon and a free carbon analysis is not yet available, so a carbide phase composition cannot be directly determined. However, high purity single crystals of "B_4C" containing no observable excess graphite are available which have been shown to have the stoichiometry B_4C. The lattice parameter for that material is essentially the same as for the powder used in the neutron diffraction target, implying that the carbide phase compositions are the same, i.e., B_4C.

Both density and composition require that an additional eleven B atoms and one C atom be contained in the unit cell. No diffraction effects were noted in the current study that indicate that any crystallographic positions are occupied other than those in the central chain and the icosahedral group. Preliminary results from the single crystal x-ray study that is in progress at LASL also indicate this to be the case.[9] The implication of this is that the icosahedral groups are, on the average, occupied by eleven B atoms and one C atom, rather than twelve B atoms as originally proposed.

The existence of a carbon atom within a B icosahedral group is not without precedent. For example,

carboranes are known that have been shown by NMR measurements to contain (B_4C) icosahedral groups.[10] It may also be noted that the replacement of such an icosahedral C atom by B logically accommodates a range of stoichiometry for boron carbide extending from B_4C toward boron rich compositions.

The accuracy of scattering amplitude determinations from either x-ray or neutron diffraction measurements is not good enough to allow the identification of one carbon atom randomly distributed within one and possibly both of the 6h position sets. The direct determination of the configuration of the icosahedral group will apparently require the use of a technique other than x-ray or neutron diffraction, e.g., NMR or possibly ESR.

3. Mass Spectrometric Studies of the Vaporization of Pu Compounds
(R.A. Kent)

The glove box - hood enclosure assembly for the Hitachi RM6-K mass spectrometer has been received. The apparatus is complete except for the sliding door assembly for the hood, which will enclose the Knudsen cell and ion source regions. This door assembly is currently being designed at LASL.

Previous calibration experiments with the RM6-K mass spectrometer indicated that the unit performed satisfactorily except that low voltage-appearance potential studies could not be performed because the emission current could not be regulated at potentials below 10 volts. The ion source is being modified into a Fox-type source. This modification should allow the measurement of appearance potentials down to 5 eV with uncertainties of ±0.1 eV.

The installation of the Hitachi unit in the glove box assembly will necessitate some changes in the vacuum system. All components necessary for these changes are on hand or are being fabricated. As these modifications are made on the vacuum system, a vacuum-measuring and protection interlock system, employing standard U.S. Bayard - Alpert ionization gauges, will be installed.

It is expected that the installation of this unit will be completed before the end of FY-1971. This instrument will be used primarily to study the vaporization behavior and thermodynamic properties of fuel components and fission products when high resolution in the high mass ranges is required.

The study of the Pu-C system has been completed and the results have been published. A future study will be of the vaporization behavior of the ternary Pu-U-C system, with particular emphasis on the composition $U_{0.8}Pu_{0.2}C$.

The existing quadrupole unit will be used primarily for the study of post-irradiated materials. These investigations will allow the determination of the identities and relative amounts of fission products present, and, more important, the obtainment of information on the chemical form of specific fission products as they actually occur in typical specimens of irradiated fuels. The study of vapor pressure and vapor species identities will make it possible to define more positively the temperature regions of importance and mechanisms by means of which vapor phase transport of fission products occurs. In addition to information on fission products per se, the effect of the fission products and chemical restructuring during irradiation on the thermodynamic activity and vapor phase mobility of the basic fuel components can also be assessed. These studies will be integral in the sense that the actual system of interest is treated. This avoids the uncertainties involved in the mathematical synthesis of overall property effects from data on abbreviated simulations of irradiated materials. These studies will necessitate a number of changes in the Knudsen cell assembly. The oven assembly for the quadrupole unit is being redesigned to incorporate a radiation shield consisting of a 1 in. thick cylinder of U^{238} metal, mounted on the inside wall of the vacuum system.

The first area to be investigated using irradiated materials is the location and mobility of tritium in both fuel and clad. Tritium is found during irradiation by an (n, T) reaction with ^6Li which is present as a low level impurity in the fuel, and is also a product of ternary fission. The primary question is the location of the tritium after irradiation, i.e., does it diffuse out of the fuel during operation and, if so, does it diffuse through the clad and enter the primary sodium coolant. This

information is necessary to allow for trapping from either fuel reprocessing effluents or the sodium coolant during operation. Both fuel and clad will be examined from irradiated pins that have been operated at both high and low power ratings to cover the range of anticipated operating temperatures.

4. High Temperature Calorimetry
(D. G. Clifton)

A number of measurements have been made using the high temperature drop calorimeter in the LASL hot cells. Six electrical calibrations of the calorimeter (taken with an empty tungsten sample capsule in the block) have given an energy equivalent of 2376.4 calories/mv with std. dev. ±.26%. An "apparent" enthalpy curve, $H_T - H_{298}$ in calories/gm, based on this energy equivalent has been constructed from six data points taken on a typical tungsten capsule. The temperatures for the data are 1198, 1348, 1461, 1582, 1641, and 1811°C. The term "apparent" enthalpy is used since these values include the radiative heat losses that occur during the drop. Ostensibly, the same losses will occur during drops of the capsules containing "unknown" samples. The effect of such losses on actual enthalpy measurements will, therefore, be removed when these tungsten data are used to correct for the heat content of the capsule.

A number of observations have been made on a 40.006 gm sample of an irradiated UO_2-20% PuO_2 fuel sample that has had a fast flux exposure of about 57,000 MWD/Te (NUMEC-B-9-56). Six drops for the temperatures 1195, 1330, 1368, 1473, 1539, and 1781°C have been made. These data are not yet fully reduced.

Two new self-heating curves have been taken for this same irradiated sample. In both cases the rates of temperature rise and the "convergent" temperatures were obtained. Determination of the self-heating power from the "convergent" temperature and the temperature-time rates agreed quite well. The average value obtained from the data is 6.31×10^{-3} watts/gm ± 2.7% std. dev.

An archival sample of the oxide used in the fabrication of the irradiation assembly has been received from NUMEC but has not yet been encapsulated. It will be run for comparison with the irradiated material.

Observations on the high temperature drop calorimeter that is used on unirradiated samples have been limited somewhat this quarter. Four more data points for empty tungsten capsules have been obtained and two additional electrical calibration runs have been made. One additional data point for the enthalpy of a 55.23 gm sample of $PuN_{0.944}$ has been obtained so that at the present time data are available at 1317, 1471, and 1555°C. These data have not been fully reduced.

A 35.1 gm sample of Pu_2C_3 has been encapsulated in a tungsten capsule. The capsule with sample has been x-ray radiographed and shows the capsule to be sound with a uniform weld penetration depth of about .050 in. This sample is now ready for enthalpy determinations.

5. Thermal Transport Properties
(K. W. R. Johnson and J. F. Kerrisk)

A. Thermal Conductivity

Design work has been completed for the reinstallation of the comparative type thermal conductivity apparatus in a new inert atmosphere glove box. Current schedules call for the installation of this apparatus after the installation of the thermal diffusivity apparatus.

B. Thermal Diffusivity

Design work is complete for the installation of the high temperature thermal diffusivity and electrical resistivity furnaces in an inert atmosphere glove box. All equipment is on hand and installation is in progress.

The thermal diffusivity apparatus, including the high temperature furnace, lasers, monitoring devices and associated equipment has been temporarily located in a cold lab to simulate the physical arrangement it will assume in a glove box. All systems have been assembled and tested. Attention was focused on an evaluation of the variables affecting thermal diffusivity measurements.

Investigations of the laser beam intensity distribution have continued using both photographic methods and thermal diffusivity measurements on thin specimens. It was shown that the image photographed directly with Polaroid Type 413, black and white film was that produced by the laser flash lamp and not the laser itself. To photograph the image produced by the Nd doped glass laser beam (1.06μ), infrared film and a corning 2-64 filter over the camera lens were used. Using this experi-

mental arrangement, all previously reported conclusions concerning the optical system and laser beam uniformity were confirmed.

Laser beam reflections from interior surfaces of the furnace were producing localized hot spots on the specimen surface. By careful realignment of the optical system and modification of the furnace apertures, this nonuniformity was reduced to an acceptable level.

Preliminary high temperature thermal diffusivity measurements were made with an EG and G,SG-100 photodiode. The noise/signal ratio was too large for accurate measurements with this detector at temperatures between 800 and 1500°C, so it was replaced with an RCA 7102 photomultiplier tube. With shielding, the noise level was significantly reduced. Light and radiation shields were added to the interior of the furnace to minimize the effect of stray reflections on the photomultiplier tube.

A specimen support was designed and fabricated from Ta. The adjustable support makes possible accurate sample alignment, has a minimum contact with the specimen, and is essentially light-tight.

Thermal diffusivity measurements are being made on a Mo specimen between 850 and 2000°C to allow the investigation of variables such as photomultiplier tube power supply voltages and optical configurations between the specimen and the photomultiplier.

G. Mechanical Properties
(M. Tokar)

A. Compressive Creep

Creep specimens of $(U_{0.79}Pu_{0.21})C_{1.02}$ having a sintered density of 11.8 g/cm^3 have been tested in compression at 1300, 1400, and 1500°C under pressures of 2000, 4000, and 6000 psi. The equipment and test procedures have been described in detail elsewhere.[11] In brief, solid right cylinders of the material of interest approximately 0.5 in. long and 0.4 in. in diam are heated by induction in a graphite susceptor. These specimens are compressed between two graphite rods, the load being applied by a hydraulic ram. The end surfaces of the specimens are separated from the graphite rods by thin B_4C discs to reduce carbon transfer. Until now, specimen deformation has been determined from micrometer measurements (± 0.0001 in.) made before and after each run. The hydraulic load was adjusted to compensate for the increase in cross-sectional area to provide a near-constant stress. In the future, specimen deformation will be measured continuously using an optical extensometer.

Typical creep curves are shown in Fig. 463-1. Two general observations may be made from these curves. The amount of primary creep was rather extensive; in fact, a specimen tested at 1400°C and 6000 psi underwent more than 26% compression before reaching a steady state creep condition. Also, the transition from primary to secondary creep occurred sooner and more abruptly with increasing stress. It should be noted that part of the deformation which occurred in the primary creep regions of the deformation vs. time plots might be accounted for by the low sintered density of the specimens (~ 87% theoretical) since densification of the specimen was noted during the tests. A few specimens approached 92% of theoretical density at termination of the tests. Most of the density increase occurred prior to the onset of secondary creep.

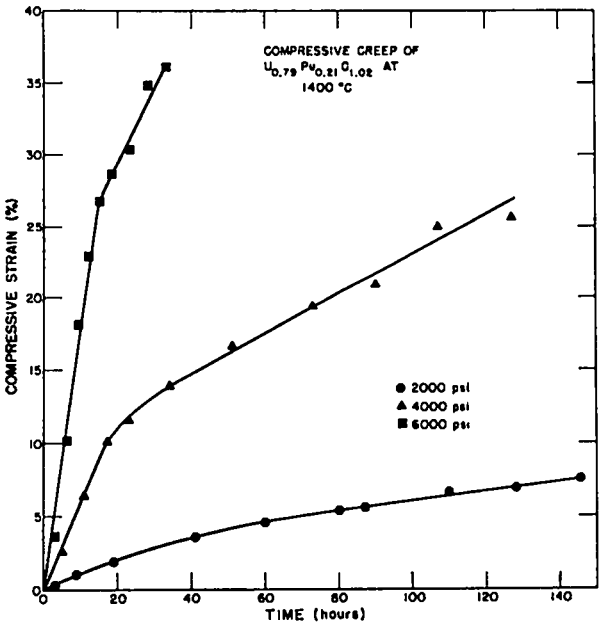

Fig. 463-1. Compressive creep of $(U_{0.79}Pu_{0.21})C_{1.02}$ at 1400°C as a function of time and applied stress.

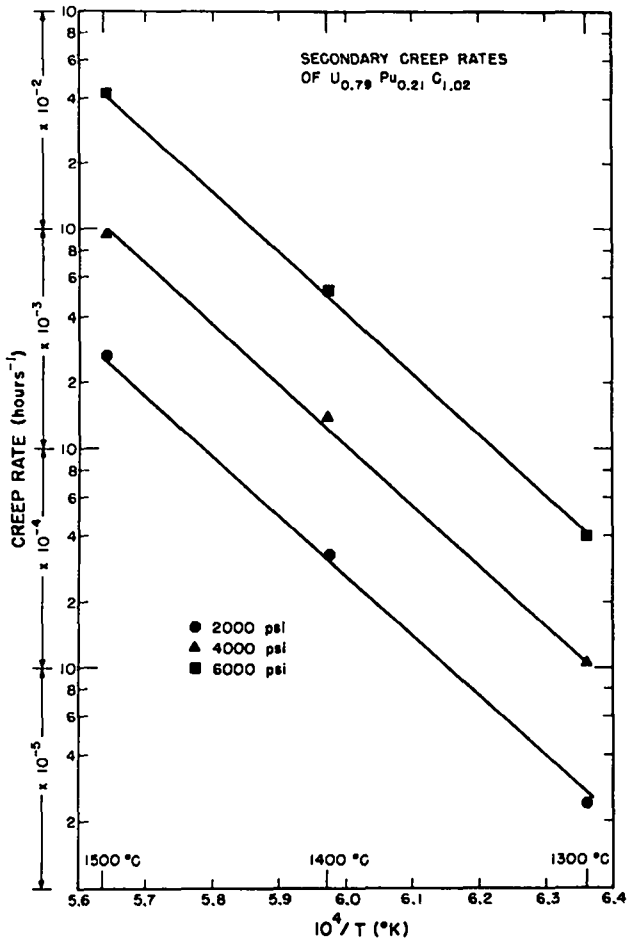

Fig. 463-2. Secondary compressive creep rates of $(U_{0.79}Pu_{0.21})C_{1.02}$ as a function of 1/T and applied stress.

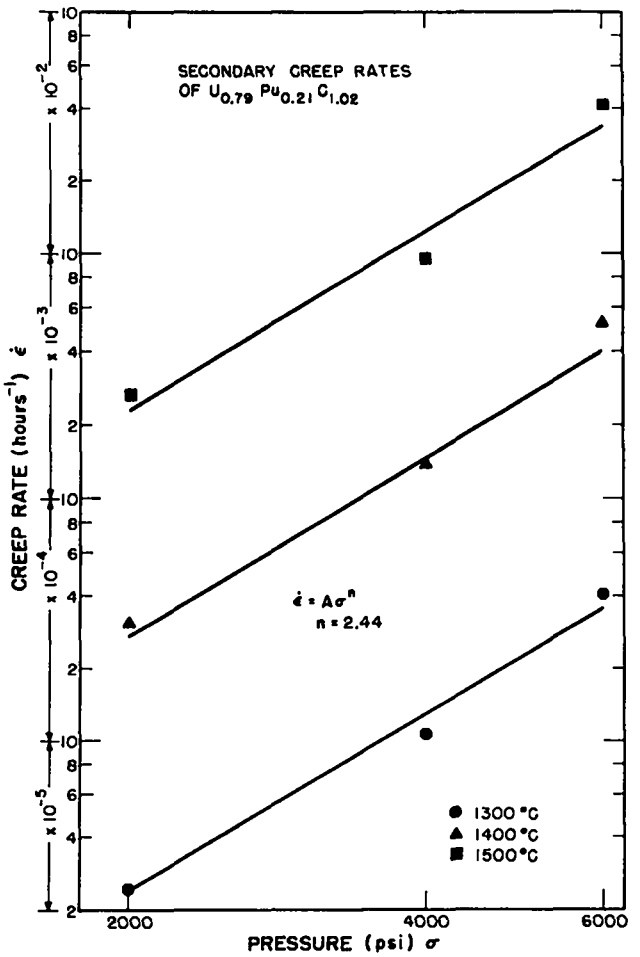

Fig. 463-3. Secondary compressive creep rates of $(U_{0.79}Pu_{0.21})C_{1.02}$ as a function of applied stress and temperature.

The effects of stress and temperature on creep rates are shown in Figs. 463-2 and 463-3. The creep data were fitted using a least squares computer program to an equation of the form

$$\dot{\epsilon} = A\sigma^n \exp(-Q/RT)$$

where

$\dot{\epsilon}$ = creep rate (hr.$^{-1}$)

A = a constant

σ = stress (psi)

n = stress exponent

Q = activation energy (kcal/mole)

R = gas constant

T = temperature (^{o}K)

The equation which best fits the data is

$$\dot{\epsilon} = 7.959 \times 10^4 \sigma^{2.44} \exp(-126/RT).$$

In a recent paper[12] the activation energy for creep of $(U_{0.85}Pu_{0.15})(C_{0.65}N_{0.35})$ was reported as 100 ± 10 kcal/mole, and in a study of creep in UC and (U, Pu)C, Killey et al.[13] reported an activation energy on the order of 100 kcal/mole for creep in $(U, Pu)C_{1+x}$. Other investigators[14-16] of creep in UC have reported activation energies between 44 and 90 kcal/mole. The activation energy for self-diffusion of uranium in UC was determined as 64 kcal/mole by Chubb et al.[17] and 104 kcal/mole by Lee and Barrett.[18] According to Stellrecht[16] the self-diffusion of uranium in UC would

be expected to be rate-controlling because uranium diffuses much more slowly than carbon. By analogy, taking into account the results of deNovion et al.,[12] Killey et al.,[13] and the present study on creep of (U, Pu)C, the self-diffusion of U (or U, Pu) would appear to be rate controlling in the case of creep of (U, Pu)C or (U,Pu)(C,N). Since the range of reported activation energies for creep in (U, Pu)C and (U, Pu)(C, N) is slightly higher than those for UC, it appears that the Pu additions may have some effect on cation diffusion in the mixed carbides, but more work is required to determine the exact nature and magnitude of this effect.

The value of the stress exponent, n, is of particular interest since it can be related to the creep mechanism. According to theory[19-21] creep by dislocation climb should yield a stress exponent of 4.5 to 5; whereas Nabarro - Herring creep (stress-directed vacancy migration) results in a linear stress dependence. Creep due to grain boundary sliding should, according to conventional theory, also result in a linear relationship between creep rate and stress. In a recent paper, however, Langdon[22] pointed out that reported examples of a linear relationship between $\dot{\epsilon}_{GBS}$ (creep rate due to grain boundary sliding) and σ are restricted to very low stress conditions and that, therefore, models which treat sliding as a Newtonian viscous phenomenon appear incapable of accounting for data obtained under the normal conditions of high temperature creep. Langdon proposed a grain boundary sliding model in which sliding occurs by the movement of dislocations along or adjacent to the boundary by a combination of climb and glide and in which the strain rate due to sliding is proportional to σ^2/d, where d is the grain size (average grain diameter). The theoretical stress exponent for this mechanism is close to the experimental value for creep in (U, Pu)C found in the present investigation and is also close to the literature values for creep in UC at 1300°C. For example, Stellrecht et al.[16] reported n=2.4, Norreys[14] reported 1.8, and Fossler et al.[15] reported 2.3. In this laboratory, ceramographic studies of $U_{0.79}Pu_{0.21}C_{1.02}$ specimens after creep testing have shown that there is very little grain strain in specimens deformed up to about 20%. This is an additional indication that grain boundary sliding is a major creep mechanism in (U, Pu)C. It is interesting to note that Stellrecht et al.[16] did obtain evidence of grain strain in UC, but in that study the size of the grains in the arc-cast specimens was about ten times that of the sintered (U, Pu)C specimens used in the present study (~ 300 μm vs. ~ 30 μm). It seems reasonable that grain boundary sliding is more likely to be predominant in specimens in which the grain size is small, i.e., in which the grain boundary area or volume is large. Thus, there may be some critical grain size below which grain boundary sliding is the predominant creep mechanism and above which dislocation climb is of major importance.

Temperature may also play an important part; although no significant variation in the stress exponent with temperature has been found in this study, Stellrecht et al.[16] reported that n increased with temperature. This would be expected if dislocation climb were becoming of greater importance with increasing temperature.

The effect of grain size on creep rate will be established in future work. If it is found that the creep rate is inversely proportional to grain size, then Langdon's grain boundary sliding theory would gain further support and the importance of grain boundary sliding in the creep of (U, Pu)C would appear to be firmly established.

The supply of samples which have been used in the creep study thus far has been exhausted. All of these specimens were prepared from one batch of material in order to avoid microstructural or compositional variations between specimens. The next series of specimens will be of higher density, since a determination of the effects of porosity on creep rate is of considerable importance.

B. Hot Hardness

Modifications of the hot hardness apparatus to allow testing at higher temperatures have been completed. Tests are now being made on carbide specimens having various U/Pu ratios. Specimens which were tested previously to a maximum temperature of 1000°C will be retested at the higher temperatures now attainable.

The apparatus has been calibrated against a Leitz

microhardness tester. Tests were made at room temperature on a block of 1020 carbon steel with a load of 200g. Results averaged about 5% lower on the hot hardness tester. This difference is probably caused by the slower loading rate of the Leitz tester which utilizes an oil-filled dash pot loading mechanism.

V. PUBLICATIONS

1. J.A. Leary, A.E. Ogard, M.W. Shupe, and J.O. Barner, "Synthesis, Fabrication, and Behavior of Single Phase U-Pu Carbides for Fast Breeder Reactors," International Meeting on Fast Reactor Fuel and Fuel Elements, Kernforschungzentrum, Karlsruhe, Germany (September 28-30, 1970).

2. J.L. Green and J.A. Leary, "The Phase Equilibria and Thermal Expansion of the Carbon Saturated Plutonium Carbides," J. Appl. Phys. 41, 5121 (1970).

3. M. Tokar, A.W. Nutt, and J.A. Leary, "Mechanical Properties of Carbide and Nitride Reactor Fuels," USAEC Report LA-4452.

VI. REFERENCES

1. F.A. Comprelli, S. Oldberg, and D. Sandusky, USAEC Report GEAP-13517 (1969).

2. H.C. Honeck, "ENDF/B, Specifications for an Evaluated Nuclear Data File for Reactor Applications," BNL-50066 (T-46), Brookhaven National Laboratory (1966).

3. R.E. Schenter, J.L. Baker, and R.B. Kidman, "ETOX, a Code to Calculate Group Constants for Nuclear Reactor Calculations," BNWL-1002, Battelle Northwest Laboratory (1969).

4. W.W. Clendenin, "Calculation of Thermal Neutron Diffusion Length and Group Cross Sections: The Glen Program," LA-3893, Los Alamos Scientific Laboratory (1968).

5. K.D. Lathrop, "DTF-IV, a FORTRAN-IV Program for Solving the Multigroup Transport Equation with Anisotropic Scattering," LA-3373, Los Alamos Scientific Laboratory (1965).

6. C.E. Dickerman et al., USAEC Report ANL-6458 (1962).

7. "Quarterly Status Report on the Advanced Plutonium Fuels Program, April 1 to June 30, 1970 and Fourth Annual Report, FY 1969," LA-4494-MS, Los Alamos Scientific Laboratory (1970).

8. H.K. Clark and J.L. Hoard, J. Am. Chem. Soc. 65, 2115 - 2119 (1943).

9. A.C. Larson, Los Alamos Scientific Laboratory, Private Communication.

10. R.E. Williams, "Carborones," Progress in Boron Chemistry, Vol. 2, R.J. Brotherton and H. Steinberg, Eds., Pergammon Press (1970).

11. M. Tokar, A.W. Nutt, and J.A. Leary, "Mechanical Properties of Carbide and Nitride Reactor Fuels," LA-4452, Los Alamos Scientific Laboratory.

12. C.H. deNovion, B. Amice, A. Groff, Y. Guerin, and A. Padel, "Mechanical Properties of Uranium and Plutonium-Based Ceramics," Plutonium 1970 and Other Actinides, Part 1, W.N. Miner, Ed., Proceedings of the 4th International Conference on Plutonium and Other Actinides, Santa Fe, New Mexico, pp. 509-517 (October 5-9, 1970).

13. N.M. Killey, E. King, and H.J. Hedger, "Creep of U and (U, Pu) Monocarbides in Compression," AERE-R6486, Presented at the 4th International Conference on Plutonium and Other Actinides, Santa Fe, New Mexico (October 7, 1970).

14. J.J. Norreys, "The Compressive Creep of Uranium Monocarbide," Carbides in Nuclear Energy, Vol. 1, Harwell, England (1963).

15. M.H. Fossler, F.J. Heugel, and M.A. DeCrescente, "Compressive Creep of UC and UN," PWAC-482 (1965).

16. D.E. Stellrecht, M.S. Farkas, and D.P. Moak, "Compressive Creep of Uranium Carbide," J. Am. Ceram. Soc. 51(8), 455-458 (1968).

17. W. Chubb, R.W. Getz, and C.N. Townley, "Diffusion in Uranium Monocarbide," J. Nucl. Mater. 13 (1), 63-72 (1964).

18. H.M. Lee and L.R. Barrett, "Measurements of Self-Diffusion in Uranium Carbide and Their Application to Related Activated Processes," Proc. Brit. Ceram. Soc. 7, 159-176 (1967).

19. J.R. Weertman, "Theory of Steady-State Creep Based on Dislocation Climb," J. Appl. Phys. 26 1213 (1955).

20. F.R.N. Nabarro, "Deformation of Crystals by Motion of Single Ions," Rept. Conf. Strength of Solids, University of Bristol, 75 (1948).

21. C. Herring, "Diffusional Viscosity of a Polycrystalline Solid," J. Appl. Phys. 21(5), 437-445 (1950).

22. T.G. Langdon, "Grain Boundary Sliding as a Deformation Mechanism During Creep," Phil. Mag. 22, 689 - 700 (1970).

PROJECT 472

ANALYTICAL STANDARDS FOR FAST BREEDER REACTOR OXIDE FUEL

Person in Charge: R. D. Baker
Principal Investigator: C. F. Metz

I. INTRODUCTION

Necessary to the development of the high quality fuel and cladding required by the LMFBR/FFTF program are reliable analytical methods for the chemical characterization of the raw materials and the manufactured fuel and for the examination of irradiated fuel.

The more immediate objectives of this project are (1) the evaluation of existing analytical methods used by potential producers of FFTF fuel, (2) upgrading those methods found to be inadequate and the development of new methods as required by additional specifications, (3) the preparation of standardized calibration materials required by various analytical methods used for specification analyses and the distribution of these materials to producers of FFTF fuel, (4) the preparation of a manual of analytical methods for FFTF fuel, (5) development of a statistically designed quality assurance program for the chemical characterization of FFTF fuel as required by commensurate specifications, and (6) provide aid, as requested, for the prequalification programs of potential FFTF fuel producers.

These more immediate objectives will be continued, as required by the development of new fuel compositions for LMFBR demonstration plants and the new or additional chemical specifications that will be necessary for their characterization.

Additional objectives of this program involve studies of irradiated fuel including (1) the development of fuel burnup measurement methods based on conventional and spark source mass spectrometric determinations of actinide and fission product isotopes, (2) the development of faster fuel burnup measurement methods based on chemical analysis techniques for use for larger routine sample loads, (3) the applications of burnup methods correlated with other measurement techniques including microprobe and metallographic examination to assess the irradiation behavior of LMFBR/FFTF fuels, (4) the measurement of fission yields, and cross sections, as necessary, to ensure highly reliable burnup methods, (5) the development of analytical methods for gases including hot cell techniques for the evaluation of their effects on cladding stability, (6) the development of mass spectrometer methods, including hot cell techniques, for studies of the gas retention properties of fuels as a function of temperature-time cycling, and (7) the application of ion emission microanalysis to elucidate migration mechanisms in irradiated fuels.

II. FFTF ANALYTICAL CHEMISTRY PROGRAM

(J. E. Rein, C. F. Metz, G. M. Matlack, R. T. Phelps, G. R. Waterbury)

The LASL-prepared document "Qualification of Analytical Chemistry Laboratories for FFTF Fuel Analysis" was issued as RDT Standard F2-6. This document prescribes the course of action by which analytical laboratories establish their technical competence for the chemical characterization of FFTF fuel and provides a quality control program for the continual evaluation of the analytical data obtained during periods of fuel production in the fabrication plants and at WADCO. As part of this quality control program, calibration blends and quality control blends in WADCO-supplied matrices of uranium oxide, plutonium oxide, and uranium-plutonium mixed oxide are being prepared for all the chemical methods of analysis to be used by all participating laboratories. The preparation of these blends is proving

more difficult than was anticipated due to adverse physical characteristics of the matrix materials. The particle size of the calcined mixed oxide powder was not sufficiently fine to permit its use and pregrinding at LASL has been necessary. The self-cohesive nature of the uranium oxide powder has required the use of lengthy blending techniques to obtain homogeneous blends. The preparation of these blends including verification of their contents and homogeneity is expected to be complete in time to meet the schedule for the FTR fuel pin qualification program.

The LASL manual of analytical methods for FFTF fuel characterization is in process of final typing with completion now estimated by mid-January and distribution expected in February. As stated last quarter, the methods in this manual are comprehensive including detailed instructions for the use of the LASL-prepared calibration blends. This places the production facilities and WADCO on a common basis which is essential for minimizing between-laboratory differences.

Modifications have been completed to the laboratories in which the two mass spectrometers will be located. The mass spectrometer to be used for nuclear fuel burnup measurements is undergoing final acceptance tests at LASL. The manufacturer of the instrument for gas analysis is experiencing difficulty meeting certain test specifications which has delayed shipment. The latest set of test results received show improved performance indicating that compliance may be attained in January with subsequent shipment.

III. NEUTRON CAPTURE CROSS SECTION VALUES FOR FISSION PRODUCTS IN FAST REACTOR SPECTRA

(R. J. LaBauve(T-1), G. M. Matlack, J. E. Rein)

An important criterion to be considered when selecting a fission product nuclide as a monitor for nuclear fuel burnup analysis is its cross section for neutron capture. The desired cross section is zero so that the number of fission product atoms present in an irradiated sample is directly proportional to the number of fissions. This, in effect, means that no corrections need be calculated and applied to correct for the capture burnout of the fission product monitor; such corrections introduce uncertainty in the burnup determination.

Using a recent compilation[1] of cross section as a function of neutron energy for fission products, effective values were computer calculated for 34 stable fission products for three fast reactor spectra typical of uranium-plutonium mixed oxide fuel. The spectra are summarized in Table 472-I and the obtained cross sections are summarized in Table 472-II.

Table 472-I

Fast Reactor Neutron Spectra Used for Fission Product Cross Section Calculations

Neutron Energy, MeV	Percent of Flux Greater than Indicated MeV		
	Spectrum 1	Spectrum 2	Spectrum 3
1.3	6.0	5.3	1.5
0.8	13	11	5.0
0.5	24	19	11
0.25	49	37	27
0.10	76	61	53
0.07	83	69	62
0.025	95	86	82
0.01	99	94	92
0.005	> 99	97	96
0.001	> 99	> 99	> 99

Table 472-II

Computer Calculated Effective Neutron Capture Cross Sections for 34 Stable Fission Products for the Neutron Spectra Given in Table 472-I.

Fission Product	Cross Section in Barns		
	1	2	3
Kr-83	0.16	0.17	0.19
Kr-84	0.013	0.013	0.014
Kr-86	0.0043	0.0044	0.0046
Rb-85	0.062	0.067	0.076
Rb-87	0.0066	0.0071	0.0080
Sr-88	0.014	0.014	0.014
Zr-91	0.022	0.023	0.025
Zr-92	0.017	0.017	0.018
Zr-94	0.014	0.015	0.016
Zr-96	0.014	0.014	0.015
Mo-95	0.083	0.089	0.099
Mo-97	0.10	0.11	0.12
Mo-98	0.045	0.046	0.048
Mo-100	0.025	0.026	0.029
Ru-101	0.19	0.21	0.25
Ru-102	0.13	0.13	0.14
Ru-104	0.041	0.044	0.050
Xe-131	0.094	0.10	0.12
Xe-132	0.048	0.049	0.053
Xe-134	0.030	0.031	0.032
Xe-136	0.0059	0.0060	0.0059
Cs-133	0.14	0.15	0.18
Ba-138	0.0035	0.0036	0.0035
Ce-140	0.017	0.018	0.017
Ce-142	0.023	0.023	0.025
Nd-143	0.096	0.10	0.11
Nd-144	0.044	0.045	0.048
Nd-145	0.078	0.085	0.096
Nd-146	0.051	0.053	0.058
Nd-148	0.051	0.054	0.061
Nd-150	0.082	0.089	0.099
Sm-149	0.43	0.46	0.53
Sm-152	0.12	0.14	0.15
Sm-154	0.10	0.11	0.12

IV. INVESTIGATION OF METHODS

An important objective of this project is the development of new analytical methods and improvement of existing methods for the analysis of various raw materials and fuels in the FFTF program. Major accomplishments this quarter are presented in this section.

1. Isotope Abundance Measurements of Uranium and Plutonium

(R. M. Abernathey, G. M. Matlack, J. E. Rein)

A rapid procedure using a single ion exchange column has been developed for the sequential separation of plutonium and uranium. The separated fractions then are analyzed for isotope abundances by thermal ionization mass spectrometry. The method basically was developed for application to uranium-plutonium mixed oxide fuel but also is applicable to other mixed-uranium-plutonium fuels as well as to the raw materials for these fuels, especially ceramic grade plutonium dioxide or plutonium nitrate.

The major steps in the separation procedure are a fuming of a small aliquot of the dissolved sample (usually in nitric-hydrofluoric acid) with perchloric acid to oxidize plutonium (and uranium) to the (VI) oxidation state, transfer of the resulting solution in 12M HCl to a highly cross-linked (10X) anion exchange resin column, elution of the americium in the nonabsorbed (111) oxidation state with 12M HCl, elution of the plutonium with a 12M HCl-0.1M HI mixture in which the plutonium reduces to the nonabsorbed (III) oxidation state, elution of the uranium (VI) with 0.1M HCl.

The separation factors for americium and uranium in the plutonium fraction are 300 and $> 1 \times 10^5$ which permits the isotopic abundance measurement of ^{241}Pu and ^{238}Pu along with the ^{239}Pu, ^{240}Pu, and ^{242}Pu isotopes. In the mixed oxide fuel specified for FFTF, for example, the ratio of $^{241}Am/^{241}Pu$ in the separated plutonium fraction is < 0.001 and the ratio of $^{238}U/^{238}Pu$ is < 0.02.

This method will be included in the LASL manual of analytical methods for FFTF fuel characterization.

2. Sequential Separation of Plutonium, Uranium, and Neodymium for Burnup Measurement

(R. M. Abernathey, G. M. Matlack, J. E. Rein)

Stable fission product ^{148}Nd with nearly equal fission yields for ^{235}U and ^{239}Pu in fast reactor spectra (as well as thermal reactor spectra)[2] is a recommended monitor[3] of total fissions in mixed uranium-plutonium fuels. In irradiated fuel samples, relative (percent) burnup is most accurately measured based on analyses for ^{148}Nd and the post-irradiation quantities of uranium and plutonium isotopes.

Several sequential separation methods have been reported in which fractions of these three elements are obtained which then are analyzed by thermal ionization mass spectrometry. These methods are characterized by lengthy procedures involving as many as five distinct separation operations.

A more rapid procedure, involving only two separation operations, is being developed for the separation of plutonium, uranium, and neodymium. The first operation is the ion exchange procedure described in the previous section which gives separated fractions of plutonium and uranium. Neodymium is in the first effluent from the ion exchange column, together with americium, other lanthanides, and various fission product and impurity elements. The neodymium then is chromatographically separated on a second anion exchange resin column. The medium for this separation is dilute nitric acid in methanol suggested by the ASTM method of Rider[4]. More optimum conditions are being developed for this chromatographic separation with objectives of high neodymium purity and speed of separation.

3. Determination of Sulfur

(G. C. Swanson, R. G. Bryan, T. J. Romero, G. R. Waterbury)

Spectrophotometric measurement of sulfur as Lauth's Violet, following separation from UO_2, PuO_2, or $(U,Pu)O_2$ by distillation as H_2S, proved to be satisfactory for determining this recently added FFTF fuel specification. The samples are dissolved by repeated evaporations with HNO_3-HF or in HCl at 325°C in a sealed tube[5], and higher oxidation states of sulfur are reduced in boiling HI-H_2PO_3 to H_2S which is distilled into a Zn $(C_2H_3O_2)_2$ solution. The resulting ZnS is reacted with $FeCl_3$, HCl, and p-phenylenediamine to form Lauth's Violet. The amount of sulfur is calculated

from the absorbance of the Lauth's Violet at 595 nm using a standard curve prepared from data obtained by analyzing known quantities of K_2SO_4 added to solutions of U, Pu, and U plus Pu.

Preliminary reduction of NO_3^- with formic acid and of Pu(IV) and (VI) with NH_2OH was found to preserve the reducing strength of the HI-H_2PO_3 mixture and ensure quantitative recovery of sulfur. The standard deviation for a single determination of 5.5 to 57 μg of sulfur is 2.8 μg of sulfur in a 0.5-gram sample (11 to 114 μg/g concentration range) and 1.8 μg of sulfur in a 0.1-gram sample (55 to 570 μg/g). Of the impurities for which maximum concentrations in FFTF materials have been specified, Fe, Mo, Ni, Ta, Ti, Al, B, Na, Co, Cd, Ca, and K at twice their specified maxima do not cause interference. Analyses are now being made of sulfur in the presence of the remaining specification impurity elements, but none of these is expected to cause interference. These analyses will conclude the testing of this method.

4. Determination of Carbon
(C. S. MacDougall, M. E. Smith
G. R. Waterbury)

Analyses for carbon in oxides of uranium, plutonium, and uranium plus plutonium by igniting the oxides at 1000°C in O_2 for 10 min and manometrically measuring the CO_2 produced were shown previously to be reliable if the samples were finely ground. Low results were obtained for unground oxides, and preliminary tests gave some indication that grinding in a CO_2-free atmosphere might be necessary. In subsequent tests, however, the amount of carbon found by repeated analyses of $(U,Pu)O_2$ pellets that were ground in air was equal to the 45 μg/g of carbon measured on samples from the same lot of pellets that were ground in an atmosphere of Ar. In other tests, (see Table 472-III) six measurements of carbon were made on each of the following materials prepared from one lot of $(U,Pu)O_2$ pellets: (1) unground chunks, (2) powder ground in Ar, (3) powder exposed to air for 1 week, and (4) powder exposed to air 1 week and reground in air. The results showed that low values were obtained for the chunks and that exposure of the ground sample to air for 1 week caused a very small pickup of carbon. Regrinding in air did not affect the carbon content.

Table 472-III

Carbon Found in One Lot of $(U, Pu)O_2$ Pellets Following various sample Preparations

Sample	Determinations	C Content, μg/g
Chunks	6	10
Powder		
Ground in Ar	6	35
Exposed to Air 1 week	6	45
Reground in Air	6	45

Increasing the ignition temperature to 1300°C during repeated analyses for carbon in $(U,Pu)O_2$ powder samples did not increase the amount of CO_2 evolved. A temperature of 1000°C, therefore, was considered adequate to burn the carbon in a ground oxide sample.

It was concluded from these results that oxides must be ground prior to measuring carbon and that the grinding could be done in air if exposure to air was minized by making the analysis as soon as possible following grinding.

5. Determination of Phosphorous
(R. G. Bryan, T. Romero, G. R. Waterbury)

Measurement of phosphorous at low concentrations in PuO_2, UO_2, and $(U,Pu)O_2$ is necessary to ensure that the specified maximum of 100 μg p/g in FFTF fuel materials is not exceeded. Analyses of solutions of the oxides is accomplished by reacting the phosphorous with $(NH_4)_2$ Mo O_4 to form phosphomolybdic acid which is extracted into n-butanol, reduced with $SnCl_2$, and measured spectrophotometrically at 725 nm. The phosphorous content is calculated from the measured absorbance and the average absorbance/μg phosphorous obtained for samples containing known amounts of phosphorous.

One of the main problems is the dissolution of the oxides without contamination or loss of phosphorous. Hot 15.6M HNO_3 containing a trace of HF dissolves UO_2 readily, $(U,Pu)O_2$ slowly, and PuO_2 very slowly. Dissolution in HCl at 325°C in a sealed tube[5], if this capability exists, is recommended for high-fired PuO_2. Following dissolution, the solution is fumed with HF-$HClO_4$ to remove volatile acids and Si. Fuming with H_2SO_4 causes low and erratic results.

Repeated measurements of phosphorous added at concentrations between 10 and 200 μg/g to 50 mg

samples of UO_2, PuO_2, and $(U,Pu)O_2$ showed that the method is unbiased. The relative standard deviation (1 σ) was no greater than 3% for phosphorous concentrations of 100 μg/g or more and increased to 4% at 40 μg p/g and 10% at 10 μg p/g. The Beer-Lambert Law was obeyed in the range of 0.5 to 10 μg of phosphorous (10 to 200 μg/g).

At the maximum impurity specifications for the FFTF materials, only Sn and Ta interfere with the method. These elements do not interfere when present at 0.1 of the specification maxima. The method has been used to measure phosphorous satisfactorily in several oxide samples.

6. Determination of O/M Atom Ratios
(G. C. Swanson, G. R. Waterbury)

The importance of the effects of O/M atom ratio on the behavior of oxide reactor fuels has prompted continued investigation of the problems involved in measuring this property. The recommended thermogravimetric measurement involves oxidation of a weighed sample in air at 1000°C followed by reduction at 1000°C in 92% He-8% H_2 to the dioxide product which is weighed. The change in weight is used to calculate the O/M ratio.

Development of these analysis conditions is a result of numerous tests on mechanical mixtures of U_3O_8 and PuO_2 prepared from U and Pu metals containing less than 100 ppm total detected impurities. As these mixtures may react differently during analysis than solid solution mixed oxides, evaporations of various aqueous solutions of U and Pu are being investigated to prepare solid solution mixed oxide powders. Preparations by evaporation of chloride, sulfate, perchlorate, formate, and acetate solutions have not been satisfactory because the salts either are deliquescent, decrepitate on drying, segregate on evaporation, segregate on burning, or are insoluble. Initial tests by evaporating nitrate solutions of U and Pu at room temperature produced dry salts which ignited smoothly, as the temperature was gradually increased, to form apparently satisfactory oxides. Further tests of this technique are in progress.

In order to shorten the analysis time, rapid oxidation and reduction of 50-mg samples of ground UO_2 in a thermobalance are being investigated. Preliminary results indicate that an analysis may be made in approximately one hour with a standard deviation in the O/M ratio of 0.01. Additional measurements are under way using the thermobalance.

7. Determination of Chloride and Fluoride
(T. K. Marshall, N. L. Koski)

Measurements of chloride and fluoride in FFTF reactor fuel materials are especially important because of the serious effects of halides on the corrosion rates of stainless steel cladding materials. Reliable methods exist for measuring each of the halides individually, but simultaneous measurement of fluoride and chloride was developed to reduce the analysis time. The sensitivity of the measurements of each halide also was improved. The chloride and fluoride were separated simultaneously from the oxide sample by pyrohydrolysis at 1000°C in a Ni boat and furnace tube using a flow of Ar-steam mixture that produced 8 ml of H_2O condensate in 15 min. The fluoride was measured with a fluoride specific-ion electrode in a 1-ml aliquot of the condensate. The chloride in the remainder of the condensate was reacted with $Hg(CNS)_2$ and Fe^{+3} to form $Fe(CNS)_3$ which was measured spectrophotometrically at a wavelength of 460 nm.

Repeated measurements of chloride and fluoride added as NaCl and HF to 1-g samples of oxides showed that the relative standard deviations were approximately 5% for a single determination of 6 to 50 μg Cl/g and 10% for 4 μg Cl/g. Relative standard deviations were 7% for measuring 5 to 50 μg F/g of oxide and 10% for 1 to 5 μg F/g. There was no bias. This reliability was considered adequate for the small quantities of halides measured. The method was used successfully in measuring chloride and fluoride in several U_3O_8 samples.

8. Determination of Water
(D. E. Vance and M. E. Smith)

Measurement of H_2O in FFTF reactor fuel pellets entails heating the pellet at 400°C, flushing the evolved H_2O with Ar to a moisture monitor, and integrating the monitor signal. The integrated signal is compared to those obtained for known amounts of H_2O generated by oxidation of measured volumes of H_2.

Sample handling and storage conditions prior to analyses are not adequately defined to minimize water pickup, depending upon the ambient humidity. Some uniform pretreatment of pellets is, therefore, necessary. This fact was amply demonstrated by heating a $(U,Pu)O_2$ pellet successively at 100°, 200°, 400°, and 800°C until the moisture showed that water was no longer being evolved at each temperature. A small amount of water (0.5 μg/g) was evolved at 100°C (see Table 472-IV) and

Table 472-IV
Water Evolved from $(U,Pu)O_2$ Pellets at Various Temperatures

Pretreatment	H_2O, μg/g, Evolved at				
	100°C	200°C	400°C	800°C	Total
None	0.5(9%)[a]	4.2(76%)	0.8(15%)	0.0	5.5
4 hr at 110°C, desiccate overnight	0.2(5%)	2.4(65%)	1.1(30%)	-	3.7
0.75 hr at 110°C under vacuum, desiccate overnight	0.3(6%)	1.8(38%)	2.7(56%)	-	4.8

[a]Percentage of total H_2O evolved

the remainder came off at 200° and 400°C. Other $(U,Pu)O_2$ pellets from the same lot were pretreated by either heating at 110°C for 4 h or by heating for 0.75 h in a vacuum oven. These pellets were then stored in a desiccator over $Mg(ClO_4)_2$ overnight before being analyzed similarly to the first pellet. Complete removal by the pretreatments of the water evolved at 100°C was not indicated, but the quantities retained were almost insignificant considering the precision of the measurements of 0.2 to 0.3 μg/g. The previously recommended pretreatment of heating at 110°C for 1 or 2 h followed by storage in a desiccator probably would be suitable to reduce surface water to a low and insignificant level. The variations in water content among pellets in the same lot proved to be greater than the water retained following pretreatment.

9. Determination of the Rare Earths, Dysprosium, Europium, Gadolinium and Samarium
(H. J. Burnett, O. R. Simi)

Spectrographic measurement, following TNOA (tri-n-octylamine) extraction to remove U and Pu, is being used to analyze UO_2, PuO_2, and $(U,Pu)O_2$ materials for Dy, Eu, Gd, and Sm. The U and Pu are extracted from a 6.7M HCl solution containing 0.2 g of the oxide sample and 5 mg of added H_3BO_3 into 20% TNOA in xylene in three passes. The aqueous phase containing the rare earths, added Y internal standard, and Am is heated to volatilize traces of B and ignited to remove traces of organic matter. The residue is dissolved in 1 ml of 1M HCl, and a 50 μl aliquot is evaporated onto a pair of Cu electrodes for analysis by a Cu-spark technique in an Ar atmosphere. These spectrographic measurements are based on a method reported by Ko[6], but include significant modifications, as described previously[7], to permit reliable analyses of materials containing maximum concentrations of impurities specified for FFTF fuel materials.

Samples of pure UO_2, and $(U,Pu)O_2$ were analyzed staisfactorily, bur difficulties were encountered in dissolving calibration and quality control blends containing known concentrations of 29 metallic impurities, generally added as oxides, in matrices of U_3O_8, PuO_2, and $(U,Pu)O_2$. Complete dissolution of the impurity element compounds was not attained by any acid combination tried. The most successful acid combination for dissolving blends having U_3O_8 matrices was 15M HNO_3-0.5M HF, followed by evaporation to dryness with $HClO_4$ and dissolution of most of the residue in 6M HCl. Insolubles in the residue contained Be, Si, Ti, Cr, Sn, Ta, and W, but the quantities were too small to interefere with the measurement of the rare earths. The relative standard deviations were between 5 and 10% for repeated spectrographic measurements of Dy, Cu, Gd, and Sm in the 6M HCl solution of the residue.

The presence of 1600 ppm of Am in pure PuO_2 matrices or of 400 ppm in $(U,Pu)O_2$ matrices, to which 10 to 100 μg/g of the four rare earths were added, did not seriously interfere with the spectrographic measurements. Work now in progress will evaluate the method for analyzing blends made with the PuO_2 and $(U,Pu)O_2$ plus oxides of the 29 impurity elements.

10. Determination of Metal Impurities
(J. V. Pena, W. M. Myers, H. M. Burnett, C. J. Martell, J. F. Murphy, C. B. Collier, R. T. Phelps)

Spectrographic measurements of 29 metallic impurities in UO_2, PuO_2, $(U,Pu)O_2$ were used in evaluating the purities of matrix materials supplied by WADCO

to be used for the preparation of calibration and quality control blends for the FFTF fuel production quality assurance program (See Section II). The UO_2 did not contain significant concentrations of any of the 29 elements. The powder was self cohesive and the weight gain when the UO_2 was ignited in air did not correspond to a quantitative conversion of UO_2 to U_3O_8. All of the UO_2 received was ignited at 900°C, but the resulting U_3O_8 was also self cohesive which required a more lengthy blending procedure to prepare homogeneous blends.

The ceramic grade PuO_2 had three impurity elements, Ca, Fe, and Mo, at significant concentrations between 18 and 50 μg/g. The powder passed easily through a 200 mesh screen and did not agglomerate.

Three containers of $(U,Pu)O_2$ were received. All of the material was granular and contained Mo in concentrations between 40 and 80 μg/g which were well above the desired 10 μg/g. Grinding in a WC-lined container with a WC ball on a mixer mill for 5 min reduced the particulate size sufficiently to allow about 50% of the powder to pass through a 200-mesh screen. Further grinding and screening of this oxide will be necessary before blends are made.

V. PUBLICATIONS

1. "Controlled-Potential Coulometric and Potentiometric Titrations of Uranium and Plutonium in Ceramic Type Materials", G. R. Waterbury, G. B. Nelson, K. S. Bergstresser, and C. F. Metz, LA-4537, 1970.

VI. REFERENCES

1. Report CCDN-NW/10, ENEA Neutron Data Compilation Center, France, December, 1969.
2. F. L. Lisman, R. M. Abernathey, W. J. Maeck, and J. E. Rein, Nucleonics 42, 191-214 (1970).
3. F. L. Lisman, W. J. Maeck, and J. E. Rein, Nucleonics 42, 215-219 (1970).
4. B. F. Rider, ASTM Standards, Part 30, Method E 321-69, pp 1096-1106, American Society for Testing and Materials, Philadelphia, 1969.
5. C. F. Metz and G. R. Waterbury, LA-3554, 1966.
6. WADCO Report WHAN-IR-5 Method No. 20.9, 1970.
7. Quarterly Status Report on Advanced Plutonium Fuels Program, LA-4546-MS, p. 23-24, 1970.

SPECIAL DISTRIBUTION

Atomic Energy Commission, Washington

Division of Research

D. K. Stevens

Division of Naval Reactors

R. H. Steele

Division of Reactor Development and Technology

G. W. Dunningham
D. E. Erb
Nicholas Grossman
W. H. Hannum (2)
K. E. Horton
J. R. Humphreys
R. E. Pahler
Sol Rosen
J. M. Simmons (2)
E. E. Sinclair
Bernard Singer
C. E. Weber
G. W. Wensch
M. J. Whitman

Division of Space Nuclear Systems

G. K. Dicker
F. C. Schwenk

Safeguards & Materials Management

J. M. Williams

Idaho Operations Office

DeWitt Moss

Ames Laboratory, ISU

O. N. Carlson
W. L. Larsen
M. Smutz

Argonne National Laboratory

A. Amorosi
R. Avery
F. G. Foote
Sherman Greenberg
H. J. Kittel
W. B. Loewenstein
P. G. Shewmon

Idaho Falls, Idaho

D. W. Cissel
Milton Levenson
R. C. Robertson

Atomics International

R. W. Dickinson, Director (2)
Liquid Metals Information Center

J. L. Ballif

Babcock & Wilcox

C. Baroch
J. H. MacMillan

Donald W. Douglas Laboratories

R. W. Andelin

General Electric Co., Cincinnati, Ohio

V. P. Calkins

General Electric Co., Sunnyvale, California

R. E. Skavdahl

Gulf General Atomic, Inc.

E. C. Creutz

Idaho Nuclear Corporation

W. C. Francis

IIT Research Institute

R. Van Tyne

Lawrence Radiation Laboratory

Leo Brewer
J. S. Kane
A. J. Rothman

LMFBR Program Office

D. K. Butler (Physics)
P. F. Gast
L. R. Kelman (Fuel & Materials)
J. M. McKee (Sodium Technology)

Mound Laboratory

R. G. Grove

NASA, Lewis Research Center

J. J. Lombardo

Naval Research Laboratory

L. E. Steele

Oak Ridge National Laboratory

G. M. Adamson
J. E. Cunningham
J. H. Frye, Jr.
C. J. McHargue
P. Patriarca
O. Sisman
M. S. Wechsler
J. R. Weir

Pacific Northwest Laboratory

F. W. Albaugh
E. A. Evans
V. J. Ruykauskas
W. R. Wykoff

FFTF Project

E. R. Astley
B. M. Johnson
D. W. Shannon (2)

Battelle Memorial Institute

D. L. Keller
S. J. Paprocki

Brookhaven National Laboratory

D. H. Gurinsky
C. Klamut

Combustion Engineering, Inc.

S. Christopher

U. S. Department of Interior

Bureau of Mines, Albany, Oregon

H. Kato

United Nuclear Corporation

A. Strasser

Westinghouse, Advanced Research Division

E. C. Bishop

Australian Atomic Energy Commission

J. L. Symonds

McD/sp.js: 129(100)